

EÖTVÖS LORÁND UNIVERSITY

FACULTY OF INFORMATICS

DEPARTMENT OF CARTOGRAPHY AND GEOINFORMATICS

**Land Use Land Cover (LULC) and Burn  
Severity (dNBR) changes analysis in Latakia,  
Syria visualized on Web maps.**

**Mohamed Wafik Hamoud**

student of Cartography MSc

**Prof. Gede Mátyás**

Associate Professor

ELTE Department of Cartography and Geoinformatics



Budapest, 2022

## **Abstract:**

Land Use Land Cover (LULC) is one of the most important domains to study in Remote Sensing analysis. This is due to the changes of each part of the world, whether it is a small area of a few kilometers or a big area of thousands of kilometers. It is one of the columns of remote sensing, and this can be done by supervised or unsupervised classification methods.

Latakia, which is a Syrian coastline city, was the studied area by using supervised classification in QGIS. The plugin, which helped achieve the final work, was Semi-Automation Classification. This plugin gave us a perfect classification according to three Landsat 7 images (2000-2010-2020) in five different classes (Water Bodies, Agriculture, Forest, Buildings and Bare Soil). To visualize the difference between these images, many calculations were done in Raster Calculator window to know what appeared and disappeared in our classes during these years.

Fire spread threatens everything on earth, and it is not limited to green areas. Many people lost their lives during enormous fires. Remote sensing helps detect fires after the beginning of its spread. This will be by comparing two or more satellite images before, during, and/or after the fire. Normalized Burn Ratio Index (NBR) helps to showing areas, which are affected by fires, and let people knowing the damaged areas.

In October 2020, Latakia suffered from large-areas fires, and it took more than two weeks to put out these fires after a massive destruction of forests, agricultural and residential areas. In this project, people can see a map of fires in Latakia that happened between the 9<sup>th</sup> and 25<sup>th</sup> of October 2020, where four Burn Severity degrees are represented (Low severity, Moderate-Low severity, Moderate-High severity and High severity). This was done using two Landsat 8 images (09/09/2020, 27/10/2020) after calculating the difference of NBR between them.

Last but not least, since WebGIS programming is the best way to visualize the results on a web page to let audiences from different parts of the world see them, I decided to make the next and the most important step by publishing this work on a Web-Based page using Leaflet with HTML, CSS and JavaScript web programming languages. I added two pages, one for Land Use Land Cover (LULC) changes, and the other for Burn Severity (dNBR).

# *Dedication*

I want to dedicate this thesis especially to my beloved family,  
who spares no effort to encourage me in every stage of my life.

You supported me in everything since I was young.

# Table of Contents

<b>1. Introduction:</b> .....	<b>1</b>
1.1 Background:.....	1
1.2 Country of study: .....	2
1.3 City of study: .....	3
1.3.1 General information about Latakia: .....	3
1.3.2 Geographical zones of the city:.....	4
1.4 Wildfire Infection and its spread in Latakia 2020: .....	5
1.5 Goal of the study: .....	6
<b>2. Literature Review: .....</b>	<b>7</b>
2.1 Landsat 7 satellite imagery:.....	7
2.1.2 Overview:.....	7
2.1.3 Enhanced Thematic Mapper Plus (ETM+).....	7
2.1.4 Landsat 7 ETM+ Scan Line Corrector Failure (SLC): .....	9
2.2 Landsat 8 satellite imagery:.....	11
2.2.1 Overview:.....	11
2.2.2 Operational Land Imager (OLI) and Thermal Infrared Sensor (TIRS): .....	12
2.3 GIS and Remote Sensing: .....	13
2.3.1 Geographical Information Systems (GIS): .....	13
2.3.2 Remote Sensing: .....	14
2.3.3 Change detection in Remote Sensing: .....	15
2.4 Supervised and Unsupervised Classification:.....	16
2.4.1 Supervised classification:.....	16
2.4.2 Unsupervised classification: .....	18
2.4.3 Which is better, Supervised or Unsupervised classification? .....	19
2.5 OTP (Orfeo Toolbox): .....	20
2.5.1 Overview:.....	20
2.5.2 ComputeConfusionMatrix: .....	20
2.6 QGIS Semi-Automatic Classification plugin: .....	21
2.6.1 Overview:.....	21
2.6.2 Semi-Automation Classification tools:.....	22

2.7 Normalized Burn Ratio (NBR):.....	24
2.7.1 Overview:.....	24
2.7.2 NBR Calculation:.....	25
2.7.3 Difference NBR (Burn Severity): .....	26
2.8 Web GIS Programming: .....	27
2.8.1 Overview:.....	27
2.8.2 Client and Server sides Architecture in WebGIS: .....	28
2.8.3 Client side programming languages in WebGIS: .....	30
2.8.4 Leaflet Library: .....	30
<b>3. Project workflow: .....</b>	<b>31</b>
3.1 Land Use Land Cover section: .....	31
3.1.1 Data Acquisition: .....	31
3.1.2 Classification of satellite images: .....	34
3.2 Burn Severity (Fire Infection) section: .....	42
3.2.1 Data Acquisition and preprocessing tools: .....	42
3.2.2 Normalized Burn Ratio (NBR) calculation: .....	45
3.2.3 Difference Normalized Burn Ratio (dNBR) calculation: .....	45
3.3 Generating Web-Based pages:.....	47
3.3.1 Home page: .....	47
3.3.2 Land Use Land Cover (LULC) and Burn Severity web-map: .....	48
<b>4. Results and Discussion:.....</b>	<b>52</b>
4.1 Overview: .....	52
4.2 Land Use Land Cover:.....	52
4.2.1 Areas Calculation:.....	52
4.2.2 Accuracy assessment tables: .....	53
4.2.3 Final classified maps:.....	56
4.3 Burn Severity (Fire Infection): .....	60
4.3.1 Values and Colors: .....	60
4.3.2 Affected fires areas: .....	61
4.3.3 Final Burn Severity (Fire Infection) map: .....	61
4.4 Web-Based pages: .....	63

4.4.1 Home page: .....	63
4.4.2 Land Use Land Cover (LULC) Web Page:.....	63
4.4.3 Fires Infection (Burn Severity) Web Page:.....	64
4.5 Conclusion: .....	65
<b>References: .....</b>	<b>67</b>
<b>Abbreviations: .....</b>	<b>73</b>
<b>Acknowledgement: .....</b>	<b>74</b>
<b>DECLARATION.....</b>	<b>75</b>

# *List of Figures:*

## *Chapter one*

Figure (1- 1): Syria map and borders with an inset map of the main location.....	2
Figure (1- 2): Latakia governorate map .....	4
Figure (1- 3): Latakia main districts.....	5
Figure (1- 4): Latakia Geographical zones.....	5
Figure (1- 5): Latakia eastern countryside fire.....	6

## *Chapter two*

Figure (2- 1): Landsat 7 Satellite.....	7
Figure (2- 2): Landsat 7 Scan Line Corrector (SLC) .....	9
Figure (2- 3): Landsat 7 ETM+ image before and after SLC failure .....	10
Figure (2- 4): Sample of SLC failure gab filling by colors .....	11
Figure (2- 5): Landsat 8 satellite .....	12
Figure (2- 6): Example of Spatial and Tabular data in GIS for the United States.....	14
Figure (2- 7): Active and Passive sensors .....	15
Figure (2- 8): Change detection in Remote sensing main steps .....	16
Figure (2- 9): Example of training sets .....	17
Figure (2- 10): Iterations and recalculations of clusters until finding appropriate centers.....	19
Figure (2- 11): Semi-Automatic classification user interface in QGIS .....	22
Figure (2- 12): SCP Dock window in QGIS .....	24
Figure (2- 13): NBR and SWIR wavelengths with reflectance values.....	26
Figure (2- 14): WebGIS architecture.....	28
Figure (2- 15): WebGIS 3-tiers .....	29

## *Chapter three*

Figure (3- 1): USGS Earth Explorer user interface.....	32
Figure (3- 2): Download Landsat 7 satellite image from USGS .....	32
Figure (3- 3): ETM+ Scan Line Correction error in Latakia image (2020) .....	33
Figure (3- 4): Latakia 2020 Landsat 7 image after filling nodata (gabs) values .....	34
Figure (3- 5): Atmospheric correction bands and 4-3-2 virtual band set for Vegetation .....	35
Figure (3- 6): Training Inputs on Landsat 7 satellite image of Latakia (2000).....	37
Figure (3- 7): 2010 classified image (Maximum likelihood classification) .....	38
Figure (3- 8): Compute Confusion Matrix window in OTP toolbox (Learning).....	39
Figure (3- 9): Kappa index and accuracy values for each classified image .....	39
Figure (3- 10): Added forests between 2010 and 2020 .....	42

Figure (3- 11): Removed forests between 2010 and 2020.....	42
Figure (3- 12): two Merged images 27/10/2020     Figure (3- 13): two Merged images 09/09/2020 .....	43
Figure (3- 14): Overpass-turbo user interface and code for download Latakia GeoJSON.....	44
Figure (3- 15): Landsat 8 post-fire image after clipping and atmosphere correction .....	44
Figure (3- 16): NBR (pre- fire) image                     Figure (3- 17): NBR (post- fire) image .....	45
Figure (3- 18): dNBR result before changing symbology .....	46
Figure (3- 19): Example of HTML and CSS codes in generating homepage .....	47

## *Chapter four*

Figure (4- 1): Classes values chart in 2000-2010-2020.....	53
Figure (4- 2): Classes accuracy for the studied years.....	56
Figure (4- 3): Classification in 2000 .....	57
Figure (4- 4): Classification in 2000 .....	57
Figure (4- 5): Classification in 2000 .....	57
Figure (4- 6): Forests change 2000-2010 .....	58
Figure (4- 7): Agriculture change 2000-2010 .....	58
Figure (4- 8): Water bodies change 2000-2010.....	58
Figure (4- 9): Buildings change 2000-2010 .....	58
Figure (4- 10): Bare soil change 2000-2010.....	58
Figure (4- 11): Agriculture change 2010-2020 .....	59
Figure (4- 12): Forests change 2010-2020 .....	59
Figure (4- 13): Buildings change 2000-2010 .....	59
Figure (4- 14): Bare soil change 2000-2010.....	59
Figure (4- 15): Buildings change 2010-2020 .....	59
Figure (4- 16): difference Normalized Burn Ratio .....	60
Figure (4- 17): Areas of Burn severity levels result.....	61
Figure (4- 18): Latakia burn severity map.....	62
Figure (4- 19): Home page user interface.....	63
Figure (4- 20): Land Use Land Cover (LULC) web page.....	64
Figure (4- 21): Burn Severity (Fire Infection) web page .....	65

# *List of Tables:*

## *Chapter two*

Table (2- 1): Landsat 4-5 Thematic Mapper (TM).....	8
Table (2- 2): Landsat 7 Enhanced Thematic Mapper Plus (ETM+).....	8
Table (2- 3): Landsat 8 OLI and TIRS characteristics .....	13
Table (2- 4): Confusion matrix example for many classes.....	21
Table (2- 5): Burn severity standard values according to dNBR. ....	27
Table (2- 6): Important languages information in client side WebGIS programming .....	30

## *Chapter three*

Table (3- 1): Downloaded satellite images for Land Use Land Cover change .....	32
Table (3- 2): Downloaded satellite images for Burn Severity map.....	43

## *Chapter four*

Table (4- 1): Confusion Matrix table for 2000.....	54
Table (4- 2): Confusion Matrix table for 2010.....	54
Table (4- 3): Confusion Matrix table for 2020.....	55

# **1. Introduction:**

## **1.1 Background:**

Our earth shape and cover are constantly changing. Here, you can imagine the importance of studying this point. Change detection became a very interesting subject to study in every aspect in order to know the various kinds of change that appeared during a period of time. This period can be from a few days to several years. There are two ways to get images of the study area. The first one is by using high resolution cameras on an airplane to take photos of a small part that we need to study, and this image will be in high resolution with a lot of pixels to visualize clearly what changed from the last time we use an airplane for this area to take an old image. The second method, which is the important one for our project, that helps us get a large-area of studying like a country or a city, is that many kinds of satellites can be used to collect images for a specific period. Choosing the satellite depends on the time we want to study, because these satellites were launched in different dates, and when any satellite covers the time for the previous one, the Agency of this satellite stops the old satellite service. Satellites specification varies from one to other regarding to bands, spatial resolution, revisit time (time take to get an image for the same place), coverage areas, etc...

Change detection can be used to show the differences in natural phenomenon or manmade things like: land use, land cover, fire infections and climate change, etc.... This feature is very helpful for the audiences, who have interests in seeing what happened in their time of interest in a specific area of the world. The visualization of these changes is represented in classified maps, where you can see and understand the change of interested classes. Classifications will be in different colors, and each year has its own classification. A small or a big change can happen each year. Supervised or unsupervised methods can be used for classification. In the first one, you can see areas you want to classify and determine them by yourself using different bands of a satellite for a better visualization, and take different data for each class. The second one is letting the software do the classification on its own. Here, GIS software will determine every similar areas in the satellite image as a class.

Using Open-Source WebGIS programming is the best way to visualize classification for all users just by clicking on a URL to check the classified maps (Land Use Land Cover, Fire Infection, etc...). Here the programmer can specify the extension of the area according to a specific map projection with various classified images, and add different layers, which visualize the change in this area. In addition, changes in each class can be added to layers if the user needs to see what happened to one class (the change in forests or agricultural lands between two years). Moreover, Phenomena can be represented on a web map to show locations that are affected by them. Legend must be added to let the audience understand the meaning of each color. This is the simplest way for the audience to see classified satellite images and changes without any complicated software.

## 1.2 Country of study:

Syria (figure 1-1) is a country located on the east coast of the Mediterranean Sea in the south-west of Asia on Latitude  $34.8021^{\circ}$  N and Longitude  $38.9968^{\circ}$  E. The general size of the country is around 185000 km<sup>2</sup>, with about 27 million population (2021 estimated). Beside Syria, there are many countries, Turkey to the north, Iraq to the east and southwest, Jordan to the south and Lebanon to the west. The country has 14 Governorates, where Damascus is the main capital of the country (Britannica, 1999).



Figure (1- 1): Syria map and borders with an inset map of the main location

Source: (Britannica, 1999).

Syria has a small coastline (around 180 km), which extends from Turkish borders in the north to Lebanese borders in the south. This coastline contains two governorates, which are Latakia and Tartous.

Here, you must know that the climate on the coastline is a lot different from the middle and east of Syria. In winter, there are a lot of rains on the coastline, while this will be lighter when you move to the east. According to that, you can realize that there are many green plains on the coast, but the country land becomes a desert in the middle and east of Syria, where winter is too cold with a few rains, and summer is too hot. Therefore, due to aridity in internal areas, vegetation and forests play a secondary role there and the undulating plains, which occupy the rest of the country (not coastline) are a definition called Syrian Desert (Britannica, 1999).

However, there are some exceptions in the northeast area of Syria (Al-Jazirah), which is located near Al-Hasakah and Al-Qamishli governorates and contains black soil. The second exception is near Euphrates River (Originated in Turkey and flows southeastward across the eastern part of Syria), which is the main, biggest and the only navigable river in the country, and there are many vegetation and forested areas on both sides of this river to the north, where it is divided into many sections (Britannica, 1999).

## **1.3 City of study:**

### **1.3.1 General information about Latakia:**

Latakia is a major Syrian city, which is situated on the Mediterranean coastline of Syria in the west side of the country (see figure 1-2). It has an area between 2297 km<sup>2</sup> and 2437 km<sup>2</sup>. Latakia governorate borders Turkey to the north, Tartous to the south, Hama and Idlib to the east (Kiddle Encyclopedia, 2022). The city has the largest containers port in Syria, and it is considered the main part of import and export for different areas of Syria especially Aleppo governorate, which is the industrial capital of the country (UN-habitat, 2014).

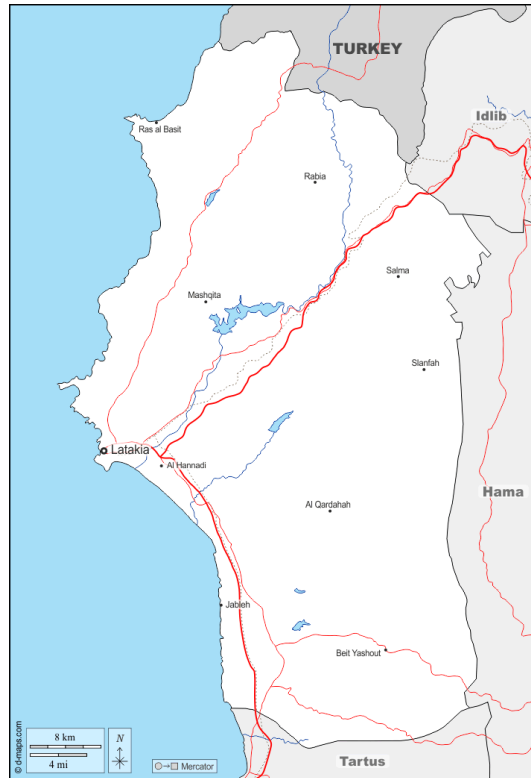


Figure (1- 2): Latakia governorate map

Source: (D-maps, 2022)

### 1.3.2 Geographical zones of the city:

Three geographical zones divide Latakia, the first one is the Coastal Zone. This is the tiniest zone and the most fertile one in the city. It is the area of the biggest cities in the governorate. The second is the mountainous zone, which has the largest area with less inhabitants. Large forested areas occupy most of this zone. The last one is Hills zone. It is located in the middle between the first two zones. This area includes secondary settlements in the village, and some of these areas became ancient sites due to migration from villages to coastal cities and Damascus (figure 1-3). The correct hills color in the figure 1-3 are light green, and mountains are light green, where there is a mistake from the source in the legend.

There are four districts of the governorate (figure 1-3 and 1-4). Beside Latakia city in the big blue point on the coastline, three orange points in figure 1-4 are the centers of the main districts of Latakia governorate. Other districts from north to south respectively are Al-Haffeh, Al-Qardaha and Jableh (UN-habitat, 2014).

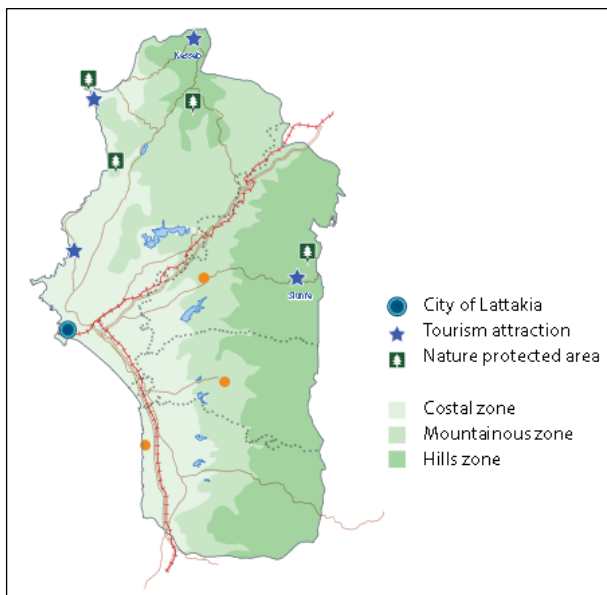


Figure (1- 3): Latakia Geographical zones.

Source: (UN-habitat, 2014)

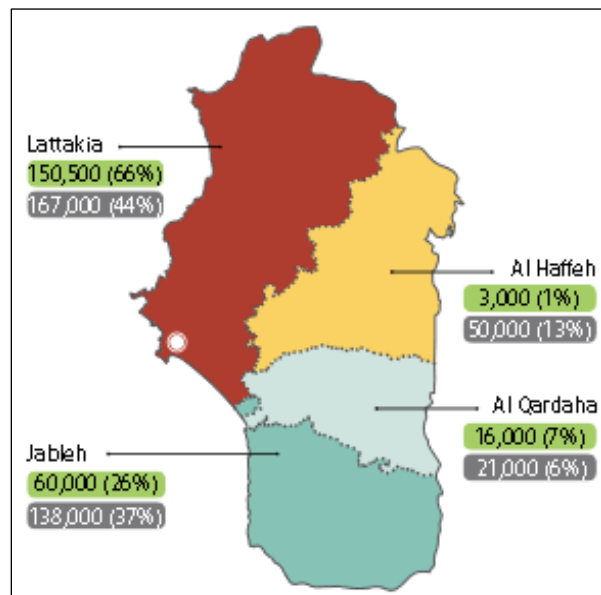


Figure (1- 4): Latakia main districts

Source: (UN-habitat, 2014)

## 1.4 Wildfire Infection and its spread in Latakia 2020:

The eastern Mediterranean Sea region had mass-destructive wildfires between October 8 and 12, 2020, which is becoming a repeating annual phenomenon due to climate change. While the origins of these flames are from many causes, enabling factors such as warm eastern breezes that are active this time of year, high temperatures, low wet trees, dried herbs and shrubs combine to generate large wildfires that consume acres of area beyond the capabilities of local authorities (IFRC, 2020).

Syria, a country destroyed by a catastrophic war, has been affected by flames killing three people and injuring approximately 80 others with respiratory problems and skin burns. Latakia province was one of the most targeted areas by these wildfires, especially in the northern countryside part. Homes, crops, forests and vegetation had been extremely affected along with many deaths and wounded citizens. Figure 1-5 represents an affected green area in the eastern countryside in latakia due to wildfires (IFRC, 2020).

According to Syrian Arab Red Crescent (SARC) report, 179 villages and forests were victims of flames, and more than 40,000 households have been impacted by injuries, temporary relocation, destruction of homes and belongings, and most importantly, livelihoods losses (trees, crops, vegetables, livestock and 30,000m of irrigation system) (IFRC, 2020).



Figure (1- 5): Latakia eastern countryside fire

Source: (Afram A., 2020).

## **1.5 Goal of the study:**

Aims and objectives are summarized in visualizing the difference in Land Use and Land Cover in Latakia between 20 years in three Landsat 7 satellite images with equal periods (2000-2010-2020) on Web-Based page after dealing, analyzing, processing and making a classification for these images using QGIS software. Then, the next step will be calculating changes in each class to represent them separately. Here, we can see and imagine what happened to five types of classes (Water bodies, Agriculture, Forests, Buildings and Bare Soil) in that period in Latakia governorate, and know the difference of areas by calculating each class area for every studied year.

The second goal is to visualize Burn Severity (fire infections) in 2020 for Latakia on another Web-Based page, where a massive fire happened in October and damaged large areas of the governorate. The process used Normalized Burn Ratio (NBR) for Landsat 8 satellite images before calculating the difference Normalized Burn Ratio to show affected fires areas. Moreover, burned areas were calculated for each burn severity level (Low, Moderate-Low, Moderate-High and high) to see how large these fires were on Latakia governorate lands.

## 2. Literature Review:

### 2.1 Landsat 7 satellite imagery:

#### 2.1.2 Overview:

Landsat 7 (figure 2-1) was launched on April 15, 1999 in Western Test Range at Vandenberg Air Force Base in California by a huge combination of the largest American involving organizations NASA, NOAA and USGS (NASA, 2019), (EOS, 2012). It was the most accurate satellite in calibration around the world, and its sensor was considered the most stable, best-characterized Earth observation instrument ever placed in orbit. First, for the usage of Landsat 7 data, user must pay a price(600\$), and this price was cheap to achieve this accurate and good quality data to work with. On October 2008, USGS made a free access to download Landsat 7 images. The repeat coverage (temporal resolution) of this satellite is 16 days for each area (NASA, 2019).



Figure (2- 1): Landsat 7 Satellite

Source: (Wikipedia, 2008)

#### 2.1.3 Enhanced Thematic Mapper Plus (ETM+)

Landsat 7 is equipped with Enhanced Thematic Mapper Plus (ETM+), which is a passive sensor (NASA, 1999). It has a ground survey in four modes: Visible and Near Infrared (VNIR), and Shortwave Infrared (SWIR), Panchromatic Range (PAN), and Thermal infrared range (TIR) (EOS, 2012). ETM+ (Table 2-1) has eight spectral bands, and it is a multispectral scanning

radiometer, which has a big advantage of providing images with high resolution and information of the Earth’s surface. When orbiting at an altitude of 705 km, ETM+ detects spectrally filtered radiation in the VNIR, SWIR, LWIR, and panchromatic bands from the sun-lit Earth in a 183 km wide swath (NASA, 2019).

ETM+ has several primary benefits (features) comparable to Thematic Mapper (TM) in previous Landsat 4 and 5 (Table 2-2), which are summarized as follows: on-board, full aperture solar calibrator, 5% absolute radiometric calibration, has a TIR channel with 60m spatial resolution, and it has a panchromatic band with 15m spatial resolution. ETM+ produces data of about 3.8 GB for each scene of the earth surface. In bands 1-5 and 7, the Instantaneous Field Of View (IFOV) of an ETM+ scene is 30 meters by 30 meters, whereas on the ground, the IFOV of band 6 is 60 meters by 60 meters. The IFOV of Band 8 is 15 meters. The scene spans 170 kilometers north to south and 183 kilometers east to west (NASA, 2019).

Landsat 7	Wavelength (micrometers)	Resolution (meters)
Band 1	0.45-0.52	30
Band 2	0.52-0.60	30
Band 3	0.63-0.69	30
Band 4	0.77-0.90	30
Band 5	1.55-1.75	30
Band 6	10.40-12.50	60 (30)
Band 7	2.09-2.35	30
Band 8	.52-.90	15

Table (2- 1): Landsat 7 Enhanced Thematic Mapper Plus (ETM+)

Source: (USGS, 2021).

Landsat 4-5	Wavelength (micrometers)	Resolution (meters)
Band 1	0.45-0.52	30
Band 2	0.52-0.60	30
Band 3	0.63-0.69	30
Band 4	0.76-0.90	30
Band 5	1.55-1.75	30
Band 6	10.40-12.50	120 (30)
Band 7	2.08-2.35	30

Table (2- 2): Landsat 4-5 Thematic Mapper (TM)

Source: (USGS, 2021).

## 2.1.4 Landsat 7 ETM+ Scan Line Corrector Failure (SLC):

Unfortunately, Landsat 7 Enhanced Thematic Mapper Plus (ETM+) Scan line corrector (SLC), which “compensates for the forward motion of the satellite” (USGS, 2008), failed on May 31, 2003. This failure caused a permanent problem regarding to satellite images, and after many unsuccessful attempts from NASA and USGS to fix it, they agreed that this failure would be existing every time. Without operating SLC (figure 2-2), the sensor’s line of sight will not be as straight lines. Instead, it will trace a zig-zag pattern all the way the satellite tracks the ground. Another issue is that there will be duplicates in scanning, which will be increased toward the edges of the satellite image (USGS, 2008).

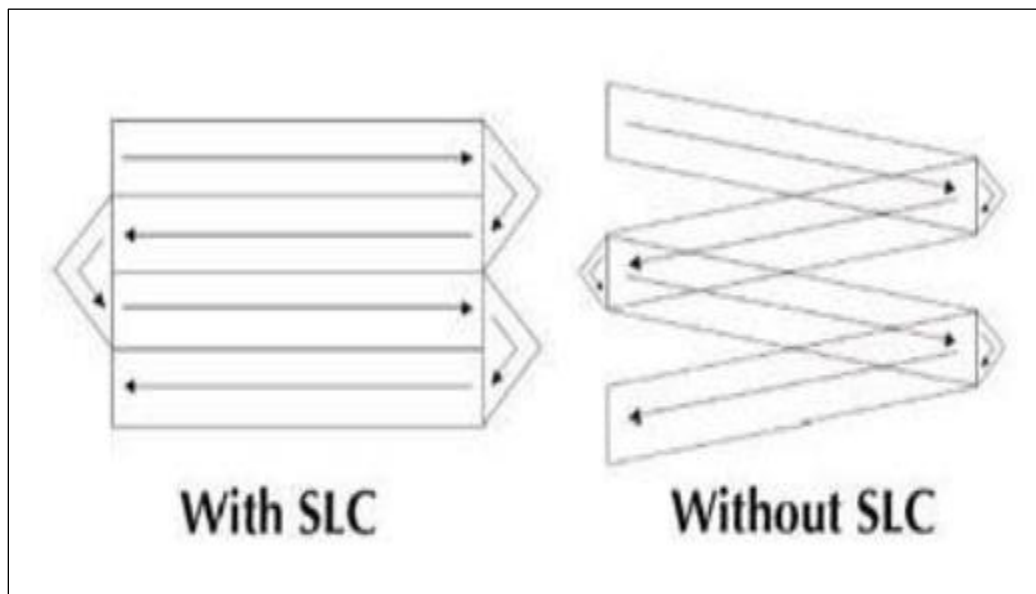


Figure (2- 2): Landsat 7 Scan Line Corrector (SLC)

Source: (USGS, SLC Failure, 2008)

After data processing, duplicates will be removed, and this will represent black stripes, which will appear continuously for many parts of the image. ETM+ continued collecting data, but with missing 22% of them due to this failure. Otherwise, these images data has the same radiometric and geometric quality as a picture, which was taken before the failure (figure 2-3). (Storey J. & Scaramuzza P. & Schmidt G. & Barsi J., 2005)

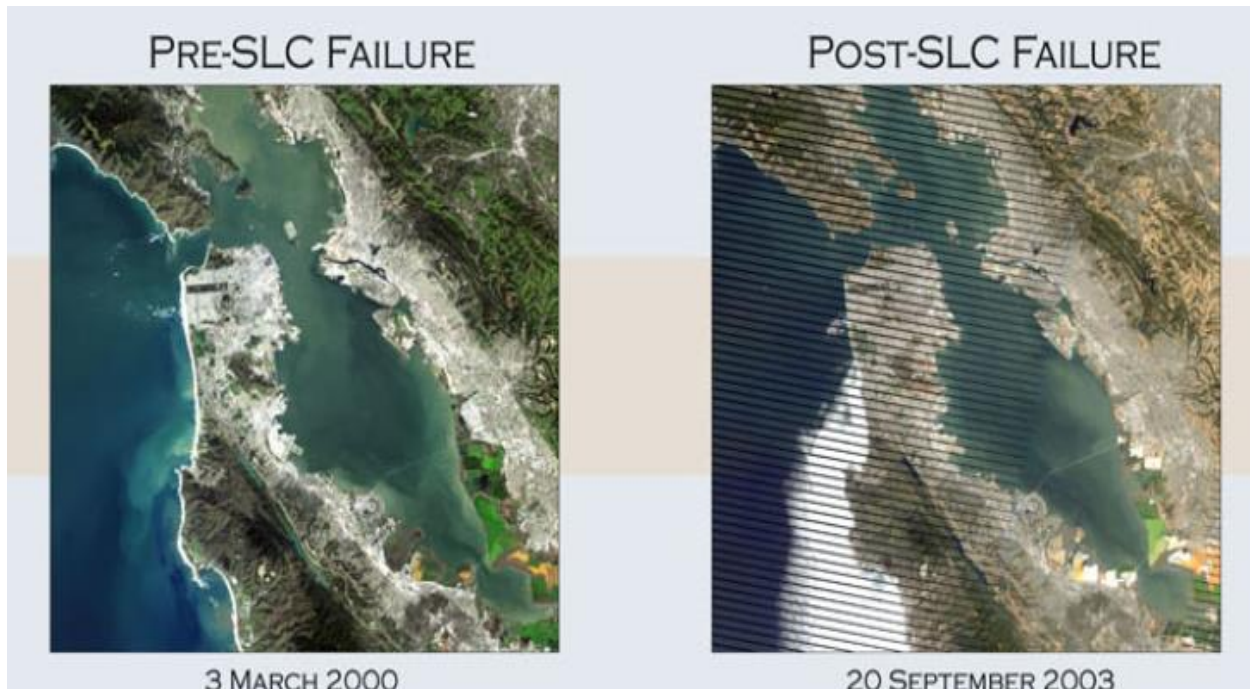


Figure (2- 3): Landsat 7 ETM+ image before and after SLC failure

Source: (Storey J. & Scaramuzza P. & Schmidt G. & Barsi J., 2005)

In order to find a solution that helps to fix this failure, in an effort to enhance the usefulness of ETM+ data obtained after the SLC failure, the USGS Earth Resources Observation and Science (EROS) Center created the infrastructure to deploy a production capability for multi-scene (same path/row) gap-filled products, using a resampling methodology. Mapping Vegetation changes applications were better to analyze after this solution if we compared this analysis to images without gap filling (black stripes in) (Storey J. & Scaramuzza P. & Schmidt G. & Barsi J., 2005). Gab-mask is given in a ZIP file (GeoTIFFs format) for each band, allowing us to fill in the data for each band independently. To see the mechanics of gab filling, look at figure 2-4 (Left: Sample SLC-Off image; Right: SLC gap mask / green: primary scene, blue: fill scene 1, red: no data (not filled)). The data values contained within the gap mask file for a conventional SLC-off product are: Zero Value – No-data (data were missing in the original SLC-off scene), and One Value– Populated-data (data were present in the original SLC-off scene) (USGS, 2008).

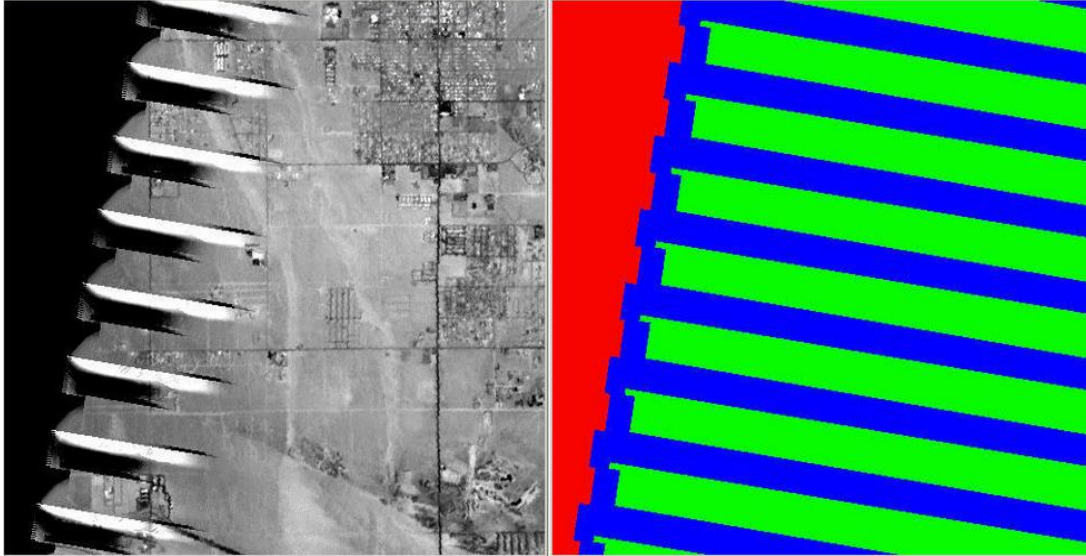


Figure (2- 4): Sample of SLC failure gab filling by colors

Source: (USGS, 2008).

## **2.2 Landsat 8 satellite imagery:**

### **2.2.1 Overview:**

As Landsat 7 neared completion, it became evident that breakthroughs in focal plane technology may allow a new class of sensors to suit the demands of the Landsat community (Knight E. J. & Kvaran G., 2014). The launch date for Landsat 8 (figure 2-5) was on February 11, 2013 from the air force base of Vandenberg, California on an Atlas-V 401 rocket, when United Launch Alliance supplied it with extended payload fairing (EPF). Two science instruments equipped with Landsat 8: the Operational Land Imager (OLI) and the Thermal Infrared Sensor (TIRS). OLI and TIRS provide sessional global landmass coverage in 30m spatial resolution for Visible, NIR, SWIR bands, 100m thermal band, and 15m for panchromatic band. Landsat 8 is orbiting at an altitude of 705 km, with a repeat coverage of 16 days (NASA, 2019).

NASA and USGS participated in the development of Landsat 8. During this time, the satellite was known as the Landsat Data Continuity Mission (LDCM), and NASA was in charge of its production, design, launch, and on-orbit calibration phases. USGS was the responsible for routine tasks on May 30, 2013, where Landsat 8 became the new name of the satellite. The routine tasks of USGS were at the Earth Resources Observation and Science (EROS) center, and these

operations were post-launch calibration, satellite operations, data product production, and data archiving (NASA, 2019).



Figure (2- 5): Landsat 8 satellite

Source: (ESA, 2022).

### **2.2.2 Operational Land Imager (OLI) and Thermal Infrared Sensor (TIRS):**

Operational Land Imager is an updated version of ETM+ in Landsat 7, and with a 185-kilometers width, it contains the technology of push-broom as well as two extra bands. TIRS also has the same technology of OLI (push-broom), and although it has two thermal infrared bands, the thermal resolution of them is less than other bands (100m while it is 15m for panchromatic, and 30m for multispectral band) (Pettinari M.L., Chuvieco E., Padilla M., Storm T., 2016). Bands 10 and 11 are both beneficial for giving more precise surface temperatures, and supporting developing applications such modeling evapotranspiration for monitoring the consumption of water usage across irrigated regions (Acharya T.D. & Yang I., 2015). High ration of signal-to-noise and a 12-bit radiometric resolution are features of OLI and TIRS. A step more than the TM/ETM+, the sensor now has two new bands: a deep-blue band for better coastal water discrimination and aerosol research, and a cirrus cloud band to achieve better results in atmospheric correction (Pettinari M.L., Chuvieco E., Padilla M., Storm T., 2016).

Level-1T (terrain corrected) consists of Landsat 8 Product. Level-1T is an unsigned integer data of 16-bit in UTM, WGS 84 projection, and image GeoTIFF format. The precision of Level-

1T is 90% for OLI and TIRS, with a circular error of 12m and 41m for these two sensors respectively. Also, Reflectance surface for atmospheric correction products are available from USGS with freely accessible in high-level data. In table 2-1, there are the characteristics for Landsat 8, where many information about each band are displayed (Pettinari M.L., Chuvieco E., Padilla M., Storm T., 2016).

Sensor	Band number	Wavelength (µm)	Spectral region	Spatial resolution (m)
OLI	1	0.43-0.45	Deep blue	30
	2	0.45-0.51	Blue	
	3	0.53-0.59	Green	
	4	0.64-0.67	Red	
	5	0.85-0.88	Near infrared	
	6	1.57-1.65	SWIR1	
	7	2.11-2.19	SWIR2	
	8	0.50-0.68	Panchromatic	15
	9	1.36-1.38	SWIR3	30
TIRS	10	10.60-11.19	Thermal Infrared1	100
	11	11.50-12.51	Thermal Infrared2	

Table (2- 3): Landsat 8 OLI and TIRS characteristics

Source: (Pettinari M.L., Chuvieco E., Padilla M., Storm T., 2016)

## 2.3 GIS and Remote Sensing:

### 2.3.1 Geographical Information Systems (GIS):

GIS is a big scientific definition. It is a technical field, where you can see a merge between geographical elements with tabular data to analyze, make maps and process in order to solve the real-world issues. The main word of GIS is Geography. This means that a part of data is spatial, and this refer to an area or a location on earth. With these spatial data, we usually have attribute data in tables (tabular data), which describe the characteristics of spatial features (Dempsey C., 2021).

For example, in figure 2-6, there is a vector map of the United States, which is spatial data with the location of each state. On the left hand side, there are attribute data (tabular data), and it contains information about each state like unique identifier (FID), polygon shape, state abbreviation, state name, FIPS code (unique code assigned to each state) and the longitude and

latitude coordinates. When you select a feature in this table, it will be selected on the map automatically in outline light blue color (California in example below).

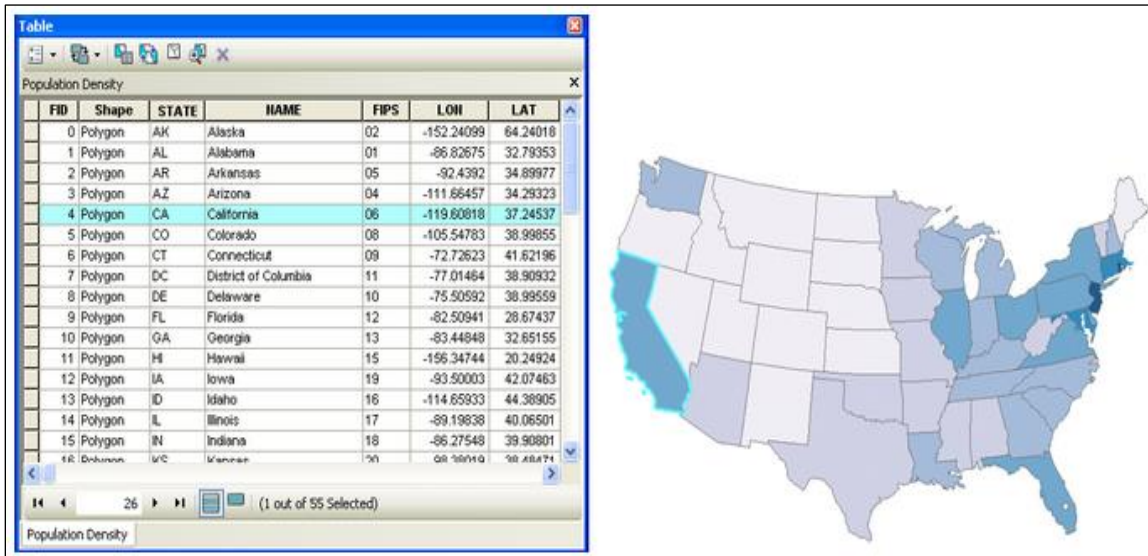


Figure (2- 6): Example of Spatial and Tabular data in GIS for the United States

Source: (Stevens J. & Smith J.M & Bianchetti R.A, 2020)

### 2.3.2 Remote Sensing:

Remote sensing is the process of detecting and monitoring the physical characteristics of an area by measuring its reflected and emitted radiation from a distance (typically from satellite or aircraft). Special cameras collect remotely sensed images, which help researchers "sense" things about Earth (USGS, 2022). Cameras can be mounted on satellite or an airplane to take images of large areas of the earth. The second type is cameras on satellites that can take images to detect temperature changes in oceans. The last type is sonar systems mounted on ships to form images of seas or oceans floor (USGS, 2022)

There are two types of sensors; active and passive (figure 2-7). Active remote sensors use their internal power to collect data. For example, using a laser-beam sensor can measure the time to reach earth and reflect back to satellite sensor by directing a laser to the earth surface. In contrast, passive sensors need an external power, and record the natural energy that is reflected or emitted from the earth surface, and the source of this energy is usually taken by the sunlight (NOAA, 2021).

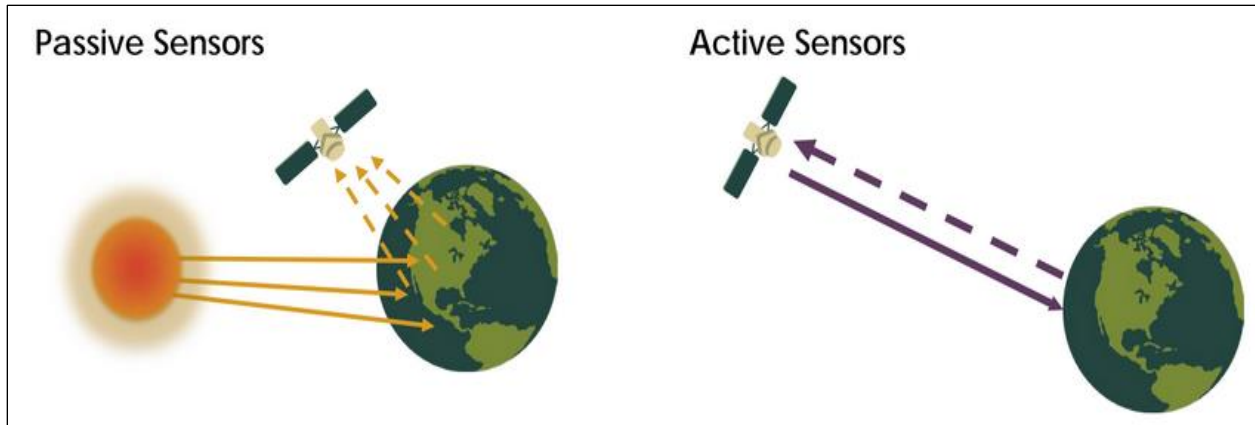


Figure (2- 7): Active and Passive sensors

Source: (NASA, 2022)

### 2.3.3 Change detection in Remote Sensing:

Remote sensing change detection is a process that allows seeing and knowing the differences of an area of the earth surface due to changes in geographical surface phenomena during a period of time (Singh A., 2010), (Panuju D.R. & Paull D.J. & Griffin A.L. ,2020). Change detection may alternatively be characterized as a technique for detecting substantial variations in successive pixel appearances caused by the presence, disappearance, movement, or form change of objects (Panuju D.R. & Paull D.J. & Griffin A.L. ,2020).

Satellite remote sensing must be used for the assessment of change detection. Land Use Land Cover (LULC), Burn Severity and other change types characteristics can be detected by these satellites, which are the main source to detect changes over time. Indeed, two types of satellites data sets are used to detect changes; the first one uses two satellite images taken in different times for the same area (bi-temporal data), and the second way is comparing a satellite image of a current or recent year, to an existing land use base map (Mohamed N. & Mobarak B., 2016).

There are many steps to reveal the change in an area (figure 2-8). Firstly, identifying the purpose and nature of change detection with area, time and classes (some classes like buildings need more than one year to be detected, while forest changes can be detected significantly between two years or more). Secondly, determine the importance of this change. Thirdly, start dealing with images to achieve the goal of this detection (Image preprocessing, choose the best change detection

algorithm, image classification, calculate accuracy to check performance) (Mohamed N. & Mobarak B., 2016).

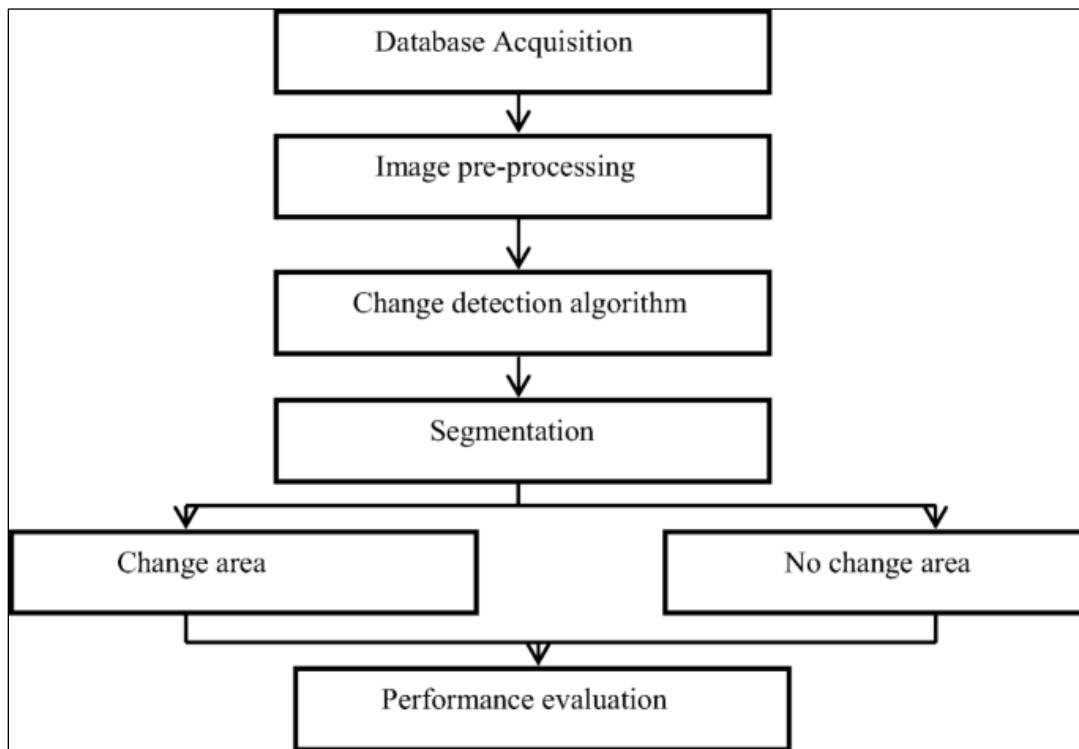


Figure (2- 8): The main steps of change detection in remote sensing

Source: (Asokan, A., Anitha, J., 2019)

## 2.4 Supervised and Unsupervised Classification:

### 2.4.1 Supervised classification:

Supervised classification is the most used technique in remote sensing image data for quantitative analysis. This method uses many algorithms, where the user must use the most appropriate one to label pixels as classes after choosing many types of classes, which the study of the image area needs for land cover (Richards, J.A., 1986). The steps of this classification are:

- Choose types of land cover that the user wants to represent on the satellite image, where many classes can be used (forests, agriculture, urban areas, water bodies, etc...)
- To classify the image, user must take appropriate pixels of each class on the image (be sure that they belong to this type). These pixels form the training data. Training sets (figure 2-

9) could be taken from the satellite image, air photographs, maps, etc.... Training fields will be on the image enclosed borders after the user chooses them (Richards, J.A., 1986).

- The next step is called calculating signature for each class, and those are sets of parameters of algorithm (Minimum distance, Maximum Likelihood, Spectral Angle Mapping) (Tumelienė E. & Visockienė J.S. & Malienė, 2021), which will be used to classify the image (Richards, J.A., 1986). Maximum Likelihood is determined as the best algorithm to study the classification of Land Use Land Cover according to accuracy and maps results (Chabaan F. & Ali A. & Mohamed A., 2020).
- Each class needs training data, and after choosing the desired trainings for land cover types, the user can classify every pixel of these data using trained classifier. Then, the whole image will be classified regarding the classes of interest (Richards, J.A., 1986).
- Finally, the user can produce thematic classes map and/or tabular data to represent and summarize the results of classification (Richards, J.A., 1986)

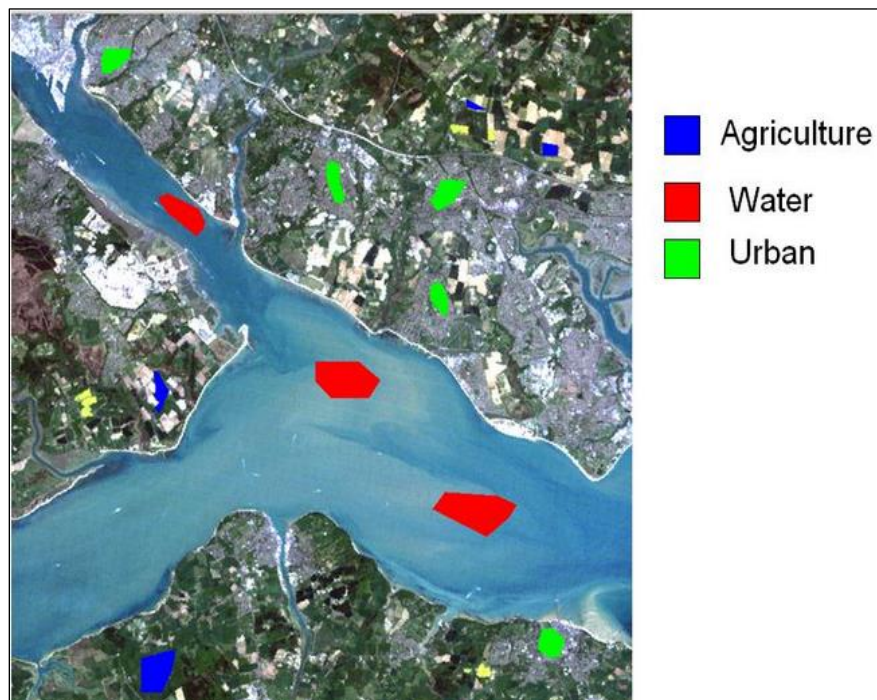


Figure (2- 9): Example of training sets

Source: [https://www2.geog.soton.ac.uk/users/trevesr/obs/rseo/supervised\\_classification.html](https://www2.geog.soton.ac.uk/users/trevesr/obs/rseo/supervised_classification.html)

## 2.4.2 Unsupervised classification:

Since supervised classification requires a knowledge of the region of interest, and if this knowledge is not in the user's hands, unsupervised classification method can be applied on the image. In an unsupervised classification, clustering algorithms are used to divide classes or features into clusters (Tempfli K. & Kerle N. & Huurneman G.C. & Janssen L.L.F, 2009).

Unsupervised classification contains several methods, and the purpose of these algorithms is unified, which is producing spectral groups according to the similarities in certain spectral data. One of the featured approaches is as follows:

- The user for the image of interest must define a maximum number of clusters (classes). So, arbitrary mean vectors will be located as the center points of the clusters by the computer.
- In the satellite image, each cell of the image will be assigned to one of the clusters by the "minimum distance to cluster centroid" rule.
- After labelling the cells, there will be recalculations of the clusters until the appropriate centers of them are found (the process iterates and stops when there is no changes in clusters), and all cells are classified (figure 2-10).
- Analysis to separate the clusters will start after clustering is finished by means of divergence measures or inter-cluster distance. The user needs to merge clusters in order to reduce unnecessary subdivisions number of classes' area (done by pre-specified threshold value if the distance between two classes is less than this value) (Tempfli K. & Kerle N. & Huurneman G.C. & Janssen L.L.F, 2009).

In unsupervised classification, number of classes, spectral distance between two classes centers, class radius, minimum number of cell are needed to eliminate clusters, which are with less than this number (Tempfli K. & Kerle N. & Huurneman G.C. & Janssen L.L.F, 2009).

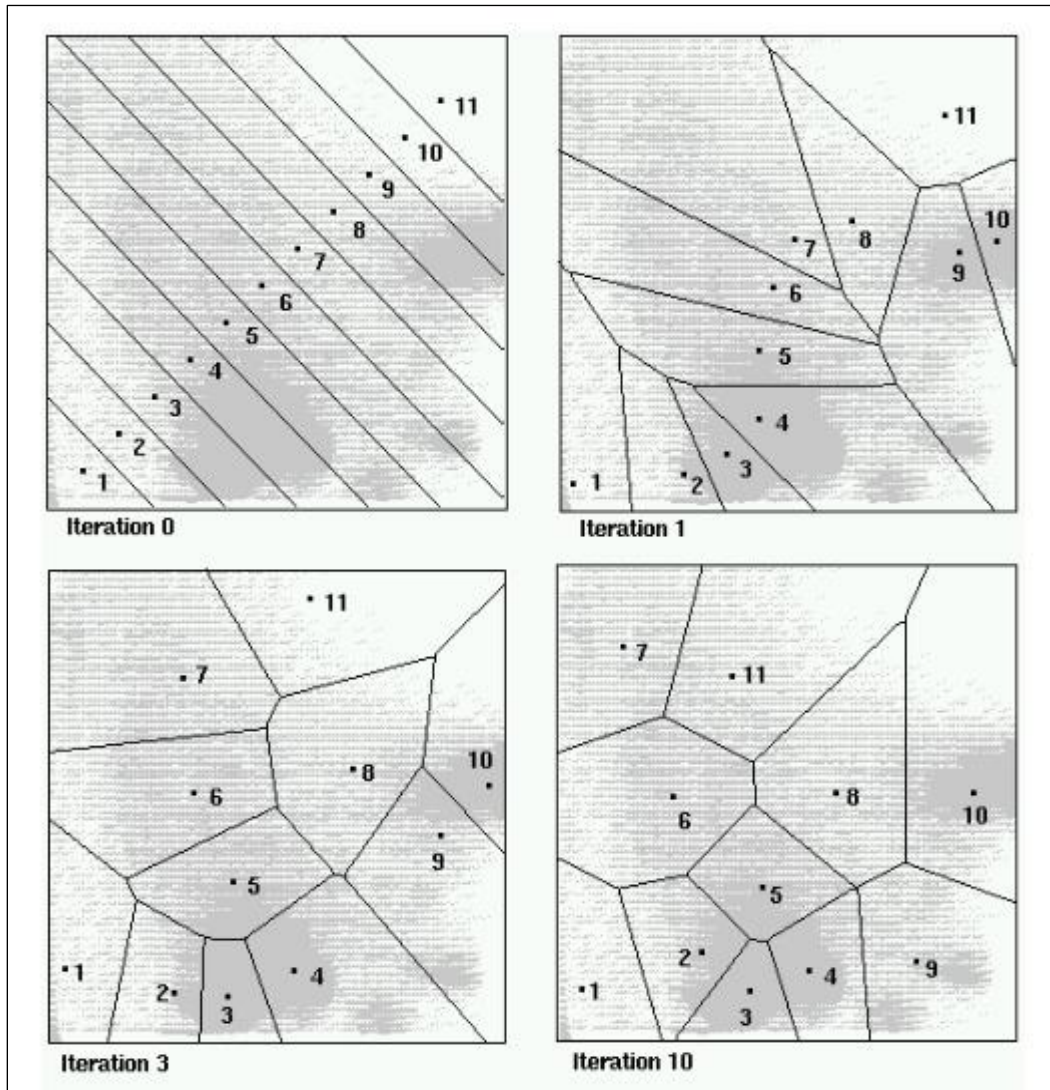


Figure (2- 10): Iterations and recalculations of clusters until finding appropriate centers

Source: (Tempfli K. & Kerle N. & Huurneman G.C. & Janssen L.L.F, 2009)

### 2.4.3 Which is better, Supervised or Unsupervised classification?

Actually, supervised classification has an advantage above the unsupervised one. It is that the user can define the important and useful classes first accurately (the user will choose training data manually from reliable images), then they will be separated after examination, while unsupervised classification will be done according to all classes, which the computer determines spectrally, and their values then will be defined (Al-doski J. & Mansor1 S.B & Shafri H.Z.M, 2013).

Besides, the user has to do something manually in supervised classification, because this type of classification needs training data, which the user must add by himself. Unsupervised classification is easy, quick to apply and does not need training data analysis; statistical software packages and image processing are widely available for this classification. It also gives us useful accurate information by converting raw image data automatically. The disadvantage is that if the user add new data, the classification process has to be recalculated (Al-doski J. & Mansori S.B & Shafri H.Z.M, 2013).

## **2.5 OTP (Orfeo Toolbox):**

### **2.5.1 Overview:**

Orfeo toolbox is an open source project used in remote sensing, and built on the shoulders of open source geospatial community. It can do many tasks with high resolution optical, Radar and multispectral images processing. There are variable applications for Orfeo toolbox, which vary between Ortho-rectification, to classification, SAR processing and compute confusion matrix, and those are Machine Learning tools (Orfeo Toolbox, 2022).

Orfeo algorithms can work on different computer systems (windows, Linux and macOS). Moreover, this toolbox is available and accessible from different platforms like QGIS, Python, Monteverdi (satellite image viewer) and C++ (Orfeo Toolbox, 2022).

### **2.5.2 ComputeConfusionMatrix:**

After classifying the map, this tool computes the confusion matrix, where the classified map is in a relationship with a ground truth dataset (user takes data according to clear areas on the ground). Vector or Raster can form and provide the ground truth dataset. No-Data values will not be recognized in the calculation of the confusion matrix (produced pixels and reference that contain data values will be computed). Confusion matrix format is: rows are reference labels and columns are produced labels (OTB CookBook, 2022). Table 2-2 shows an example of confusion matrix.

Class	Road	Building	Green	Bare	Row total
Road	101	0	25	20	146
Building	0	128	0	17	145
Green	10	0	104	1	115
Bare	2	4	2	105	113
Column total	113	132	131	143	519

Table (2- 4): Confusion matrix example for many classes

Source: (Elkhrachy I., 2015)

When numbers in the matrix (except main diagonal elements) are close to zero, it gives the class more accuracy. The single class accuracy can be calculated according to rows and columns for producer and reference by dividing the main diagonal element for each class to the sum of row or column elements for that class (these elements are assumed as false values for the class and they will reduce the accuracy). Overall accuracy equals the division of mean diagonal values on rows or columns sum value (value is equal for them).

## 2.6 QGIS Semi-Automatic Classification plugin:

### 2.6.1 Overview:

Semi-Automatic classification, which was developed by Luca Congedo in 2012, is an open source python plugin used for supervised classification in QGIS. This plugin consists of a set of intertwined tools and user interface aims to facilitate the calculation for land cover classification, from downloading satellite images, through pre-processing (prepare data before classification) and processing ( performing a classification for land cover) till post-processing (calculating accuracy, repair classification and adding additional data) (Congedo L., 2021).

Semi-Automatic classification allows the user to deal with different free available data from Landsat, Sentinel-1, Sentinel-2, Sentinel-3, MODIS, GOES and ASTER. After downloading satellite image (bands), it is easy to do pre-processing and raster calculations steps automatically by just setting a few parameters in the user interface (Congedo L., 2021). User interface window is represented in figure 2-11.

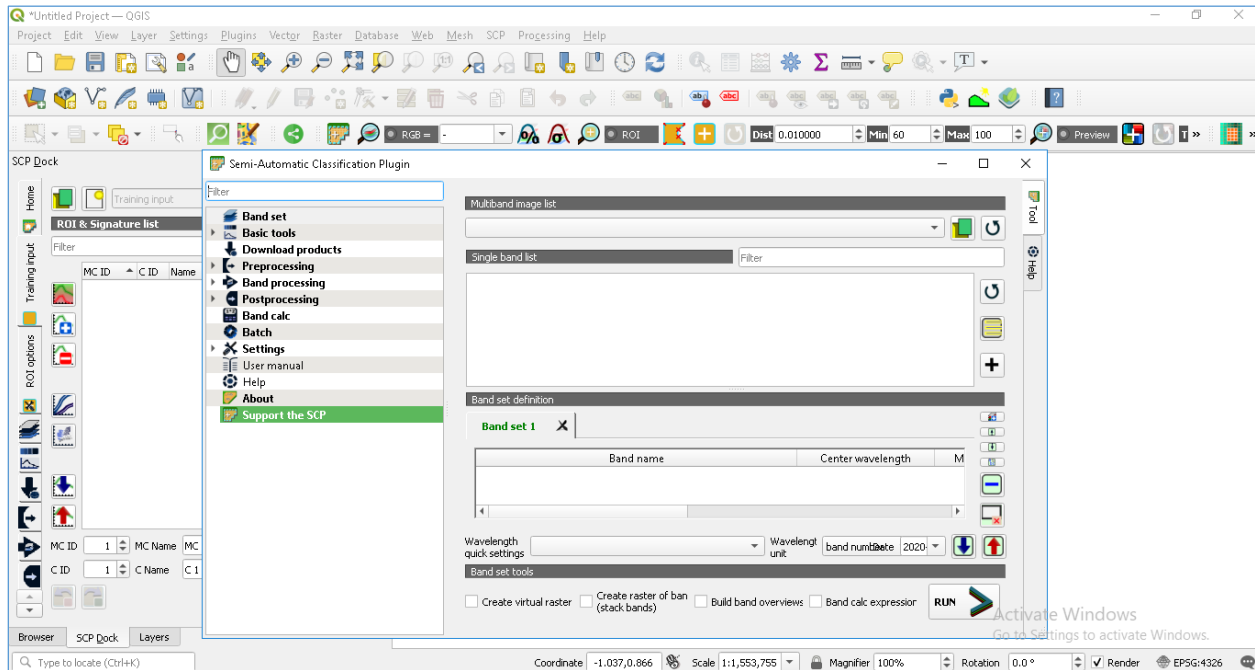


Figure (2- 11): Semi-Automatic classification user interface in QGIS

## 2.6.2 Semi-Automation Classification tools:

User must define band set (raster bands) in user interface by adding bands first to QGIS, then to Band set menu in Semi-Automatic classification (Congedo L., 2021). Many tools for pre-processing, processing and post-processing are available in this plugin:

1. Pre-processing tools:
  1. Clip multiple rasters at the same time (user can clip all satellite bands together after adding them to band set).
  2. Removing atmospheric effects (Atmosphere correction) for satellite images and converting to true surface reflectance for different types of satellites: Landsat, Sentinel-1, Sentinel-2, Sentinel-3, MODIS, ASTER and GOES.
  3. Cloud masking depending on the values of a raster mask.
  4. Mosaic band sets, merging the corresponding bands of two or more band sets.
  5. Statistic calculation for neighbor pixels

6. Re-projection of the coordinates of raster bands.
  7. Splitting or stacking raster bands in a unique file
  8. Vector to raster conversion (Congedo L., 2021).
2. Processing tools:
1. Combine bands together to achieve a raster where each band value corresponds to a combination of input values.
  2. Useful tool for clustering in unsupervised classification.
  3. Analysis of the components of band set.
  4. If there are two band sets, spectral distance between every corresponding pixel can be calculated.
  5. Get final classification by using several algorithms, such as Maximum Likelihood, Minimum Distance and Spectral Angle Mapping (Congedo L., 2021).
3. Post-processing tools:
1. After finishing the classification, the user can calculate the accuracy assessment for this image classification.
  2. Many processes for classification (erosion, dilation and sieve for refining patches of the classes).
  3. Getting a report of classification to calculate classes' statistics like area, percentage of the class and number of pixels.
  4. Convert the classification from raster to vector.
  5. Enable the user to edit raster values manually.
  6. Providing raster image for Land Cover Change, which compare between two classifications.
  7. Reclassification of raster values.
  8. Every unique value of a reference raster or vector has statistics related to input raster (Congedo L., 2021).

Since Semi-Automatic Classification needs training data for supervised classification, there is a panel the user can open from View window. This panel is called SCP Dock (figure 2-12), it allows the user to take training data, and spectral signature calculation is available. Furthermore, in SCP Dock, the user can create classification previews on a small part of the

satellite image to see and visualize the results before launching the classification for the whole image. Signatures of classes can be visualized in SCP Dock in order to assess the spectral separability of signatures. In addition, there is a band calculator in the plugin (It runs like Raster Calculator in QGIS), where the user can perform mathematical and conditional calculation using rasters.



Figure (2- 12): SCP Dock window in QGIS

## 2.7 Normalized Burn Ratio (NBR):

### 2.7.1 Overview:

To identify changes in forest structure and moisture content induced by fires, satellite data may be utilized to map burn severity (Cocke A.E, Fulé P.Z. Crouse J.E., 2005). A big group of remote sensing experts is depending on the usage of Normalized Difference Vegetation Index (NDVI) for assessing burn severity and detecting fires. Despite that, the Normalized Burn Ratio (NBR) has been considered the main index to determine fires and burn severity. In the United

States, NBR is employed as a nationwide operating tool. By integrating near infrared (NIR) and Short-Wave infrared (SWIR) reflectance, the index corresponds to vegetation vigor and moisture. NBR must be operated on two images (pre and post fire) to apply bi-temporal image differencing, where Difference Normalized Burn Ratio (dNBR) can be calculated, and its value ranges from 0 (no-burn) to 1 (high-burn) (Veraverbeke S. & Lhermitte S. & Verstraeten W.W. & Goossens R., 2010).

### 2.7.2 NBR Calculation:

Landsat 4-5 and 7 are basically used to obtain Normalized Burn Ratio (NBR), and considered special satellites for this index. Also, it may be used with any multi and hyper spectral sensor, which has 760-900 nm wavelength of Near Infrared (NIR) band, and another wavelength range between 2080-2350 nm for Short-Wave Infrared (SWIR) band. Therefore, NBR can be calculated from other satellites like Landsat 8, MODIS and others (Wasser L. & Cattau M., 2020).

NBR can detect burned areas with obtaining a burn severity measure. Values of NIR and SWIR band can calculate this index. According to Landsat satellites series, NBR can be calculated for Landsat 4-5 Thematic Mapper, Landsat 7 Enhanced Thematic Mapper Plus, and Landsat 8 Operational Land Imager (OLI) and Thermal Infrared Sensor (TIRS). The equation of NBR calculation is the subtract between NIR and SWIR bands, where it is different in Landsat 8 from other versions as follows (USGS, 2022):

$$NBR = \frac{NIR - SWIR}{NIR + SWIR} :$$

*Landsat 8: NIR = band 5, SWIR = band 7*

*Landsat 4 – 7: NIR = band 4, SWIR = band 7*

Given that vegetation reflects heavily in the NIR area of the electromagnetic spectrum (wavelength) and weakly in the SWIR, the NIR and SWIR sections of the spectrum are a potent combination of bands to employ for this index. A fire scar that includes scarred woody plants and the ground, on the other hand, has been demonstrated to reflect more strongly in the SWIR section of the electromagnetic spectrum and beyond. As a brief, vegetation reflectance in NIR is so strong;

while it is weak in SWIR band (fire effects on vegetation areas will form an increased reflectance on SWIR band and decrease reflectance for NIR band in the same burned area). With a combination of these bands results, it is easy to determine areas with fires in the studied location (Wasser L. & Cattau M., 2020). See figure (2-13) that shows reflectance and wavelengths for NIR and SWIR.

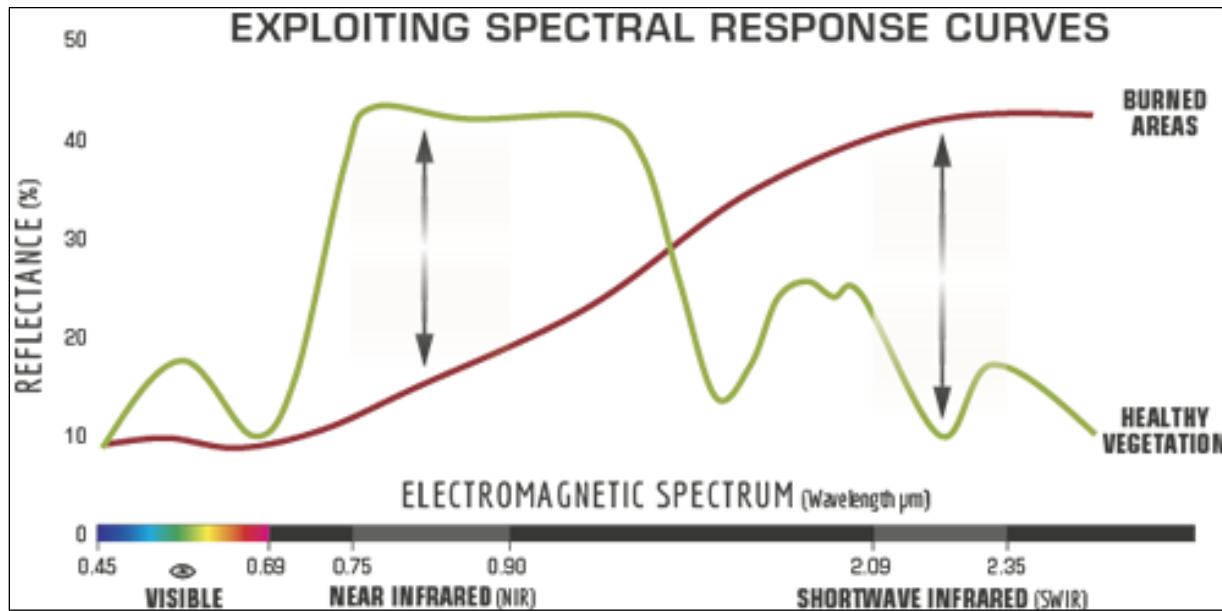


Figure (2- 13): NBR and SWIR wavelengths with reflectance values

Source: (Wasser L. & Cattau M., 2020)

### 2.7.3 Difference NBR (Burn Severity):

As mentioned above, Normalized Burn Ratio is the most effective composite to determine burn severity, but it does not end after calculating this index. After calculating NBR for two images, it is the turn to calculate Difference Normalized Burn Ratio (dNBR), which is defined as a result of the subtraction between pre-fire NBR image, and post-fire NBR image. If pre-fire image is before fire, and post-fire one is immediately after fire, the result will be the best because if plants regrow, NIR will be more reflected, and SWIR reflectance will decrease day by day. Tropical countries fires are less effective by NBR due to the nature of these areas (wet and vegetation grows fast), while in some countries like United States, NBR will give a perfect result, because of the longtime taken for crops regeneration (Wasser L. & Cattau M., 2020).

The equation of difference Normalized Burn Ratio (dNBR) calculation is represented below, and burn severity standard levels after dNBR calculation and classification are existing in table 2-3:

$$dNBR = NBR (Pre\ fire) - NBR (Post\ fire)$$

Severity Level	dNBR Range (scaled by 10 <sup>3</sup> )	dNBR Range (not scaled)
Enhanced Regrowth, high (post-fire)	-500 to -251	-0.500 to -0.251
Enhanced Regrowth, low (post-fire)	-250 to -101	-0.250 to -0.101
Unburned	-100 to +99	-0.100 to +0.99
Low Severity	+100 to +269	+0.100 to +0.269
Moderate-low Severity	+270 to +439	+0.270 to +0.439
Moderate-high Severity	+440 to +659	+0.440 to +0.659
High Severity	+660 to +1300	+0.660 to +1.300

Table (2- 5): Burn severity standard values according to dNBR.

Source: (United Nations, 2022)

## 2.8 Web GIS Programming:

### 2.8.1 Overview:

From the name of the title, everyone can realize that this definition is related to web, where WebGIS is a developed version of Geographical Information Systems (GIS) represented on web platform, and the exchange of information is between the server (GIS) and the client (Web Browser, desktop application and mobile apps). The client can find the server on the internet, because this server has a unique Uniform Resource Locator (URL). Web GIS made an ease for people to reach data without the requirement of creating custom applications. Usually, organizations use web GIS to manage their geographic data properly (VizExperts, 2022).

In other words, Web GIS programming contains creating, extending, utilizing Web mapping solutions to solve and treat specific problems, building applications, producing and consuming geospatial processing services with data. Moreover, Applications Programming Interfaces (APIs), which are offered by many options of WebGIS software, provide means by which developers can get benefits from the published data and processing services of others to

build and customize applications through standardized interfaces with external web GIS software, data, and services (Swift J. & Goldberg D., 2019). In WebGIS programming projects, commonly used open source and other paid software APIs focus on mashups. Leaflet and OpenLayers (open source), Google maps APIs, Mapbox GL JS, ArcGIS REST API, ESRI ArcGIS API for JavaScript, ArcGIS Python API and ArcGIS Runtime SDKs (software development kits) are the most popular platforms. These days, the usage of WebGIS is spreading fast, due to the popularity of internet around the world (Swift J. & Goldberg D., 2019).

## 2.8.2 Client and Server sides Architecture in WebGIS:

The client/server approach is used to implement a WebGIS. The entire activity is divided into two parts (figure 2-14): client side, and server side. Using web browser or GIS desktop software is the assignment of client side, whereas the server includes a web server (Apache Tomcat), a web GIS server (Geoserver, Mapserver), and a Database (PostGIS). To understand this approach easily, and with a normal example aside from technologies, imagine the following scenario; a customer (client) in a cafeteria wants to order something; the waiter (server) will hear the order that the customer wants to request. After the waiter gets the order, he will process it, and take it to the chef (database) to prepare the customer’s order (client request) before returning the response to the client (Jolaiya E., 2020).

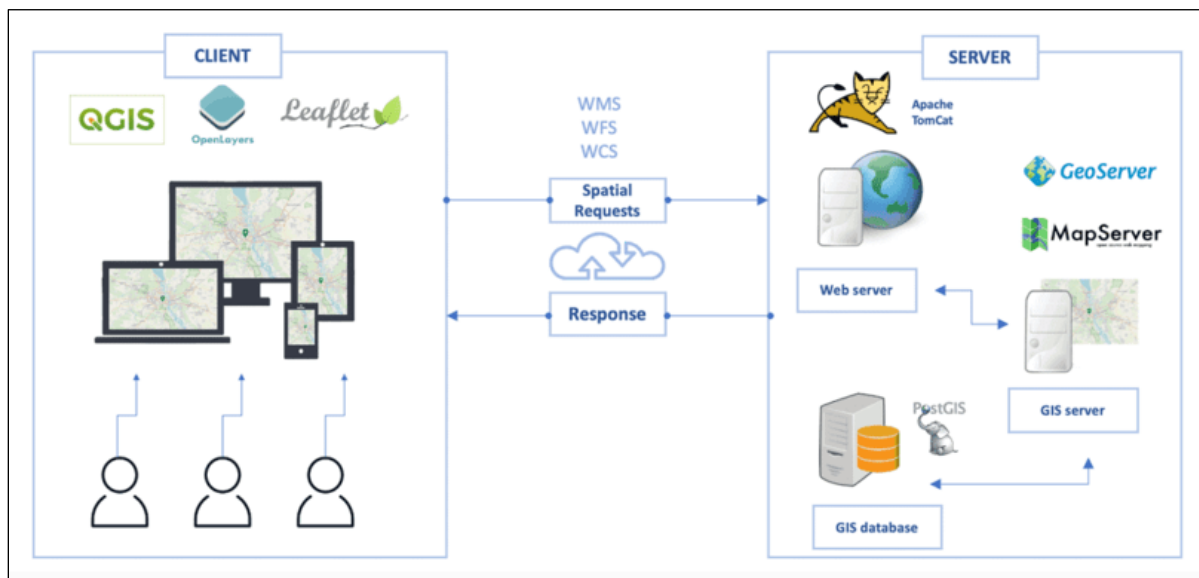


Figure (2- 14): WebGIS architecture

Source: (Jolaiya E., 2020)

In other words, WebGIS consists of three-tier architecture (figure 2-15); which are described in the following sentences:

- User Interface Tier:

This is the user intersection layer. User interface availability and efficiency are the main parameters this tier focuses on. Users can access the system using any web browser due to the feature of the system that it is prototyped over the internet. HTML, AJAX, and JavaScript are the most common web GIS languages (Tiwari A. & Jain K., 2013).

- Application Logic Tier:

This tier can be defined as a category, which contains two elements:

1. Web Server: it uses a web browser to communicate with the client. This is by the usage of the web browser and HTTP protocols to deliver web pages, and an application to the client, respectively.
2. Web Map Server: this offers tools suite for creating online mapping apps, and web services that are spatially enabled. It allows querying and analyzing the shown data, as well as accessing and displaying spatially enabled material from the geodatabase (Tiwari A. & Jain K., 2013).

- Database Tier:

All permanent data are managed via the system of database management, where information about metadata is saved and retrieved. Database tier is also in charge of handling updates, enabling concurrent access from web servers, assuring data integrity, and offering rapid and flexible access to metadata (Tiwari A. & Jain K., 2013).

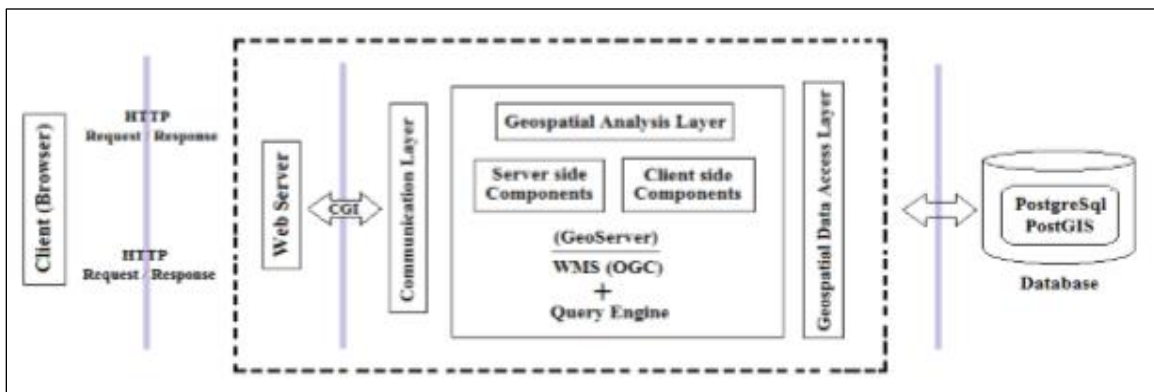


Figure (2- 15): WebGIS 3-tiers

Source: (Tiwari A. & Jain K., 2013)

### 2.8.3 Client side programming languages in WebGIS:

Client-side programming languages are used to create web pages and WebGIS applications. The most frequently used programming languages in client side are HTML, CSS and JavaScript. They control what is shown, and what happens on a web page (embedding web map in a web page is included) by working together. The client's computer is used to handle all of these languages. The next table shows some information about the most used programming languages in the client side (Swift J. & Goldberg D., 2019).

Language	Extension	Description
HTML	.html	Hypertext markup language: controls the structure and content of a web page.
CSS	.css	Cascading stylesheets: controls the look and feel of a web page.
JavaScript	.js	Scripting language used to write web GIS clients and to utilize or extend 3 <sup>rd</sup> party APIs. Can be used to create 3 <sup>rd</sup> party frameworks and libraries.

Table (2- 6): Important languages information in client side WebGIS programming

Source: (Swift J. & Goldberg D., 2019)

### 2.8.4 Leaflet Library:

The creator of leaflet in 2011 is Volodymyr Agafonkin, who comes from Ukraine. Leaflet is the most widely used open-source JavaScript library for creating mobile-friendly interactive maps. It provides all the mapping functionality most developers will ever need in just 39 KB of JS and 4 KB of gzipped CSS code. Leaflet was created with ease of use, performance, and functionality in mind. Leaflet works well on all major desktop and mobile platforms. You can utilize HTML5 and CSS3 on modern browsers while remaining compatible with older browsers. This library offers a large number of plugins, a beautiful, clean, and well-documented API, and simple, legible source code that is a delight to participate in (Agafonkin V., 2022).

## **3. Project workflow:**

### **3.1 Land Use Land Cover section:**

#### **3.1.1 Data Acquisition:**

##### **3.1.1.1 USGS Earth Explorer:**

To get the project data, three Landsat 7 satellite images were downloaded from USGS Earth Explorer (figure 3-1). USGS provides free data from different satellites. The user can search for images using specific criteria, such as the name of the area of interest (or drawing polygon or writing coordinates for this area), specifying the date and months of the image (between two dates), and managing some additional conditions like clouds cover percentage in the image. To get Landsat 7 ETM+ images, Landsat collection 1 Level-1 has been used from data sets, with land cloud cover less than 20% to make the appearance of classification clearly for the whole of our area.

To get real changes for different classes ranging from short to long-term changes together, there must be a minimum of ten years to detect this change. Satellite images in this project continued for twenty years from 2000 to 2020, where they were taken as ten years between each one respectively (2000-2010-2020). Regarding months, each image should be at the same period of the other image. This is for repeating the same season each year to avoid differences in for agriculture and forest areas due to mowing and climate changes. So, the months for these images were three (the reason is facing clouds covers in case of taking images in the same month each year), and these months are May, June and July. Actually, this will not have an affect, because according to the climate of Latakia, the whole period from the middle of April to the end of August is for agriculture growth, and mowing happens every year in the first half of September. After setting all criteria, all images according to the chosen date, cloud cover and satellite type will be shown and ready to download by one click for all bands. Bear in mind that the user can download different options of the satellite image like, natural color image, thermal bands image and others, but for classification, full image data product must be downloaded (figure 3-2 shows the download window for the image in 2000). Information about images are represented in the table 3-1. This information also contains the situation of Landsat 7 Scan Line Error (SLC), where it failed in the period between the first and second images.

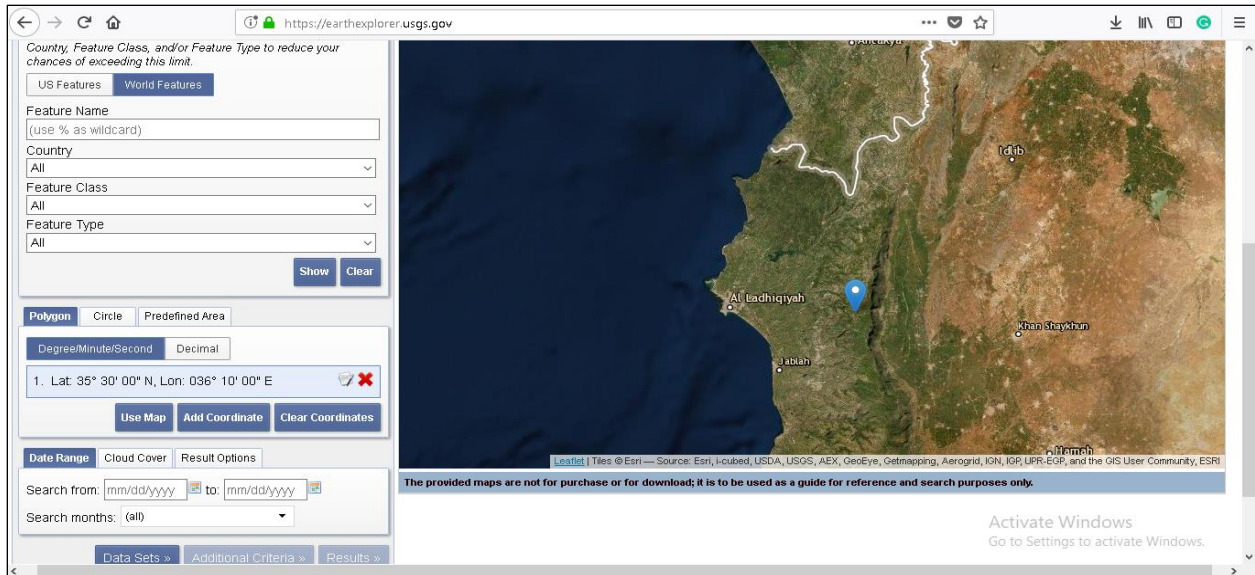


Figure (3- 1): USGS Earth Explorer user interface

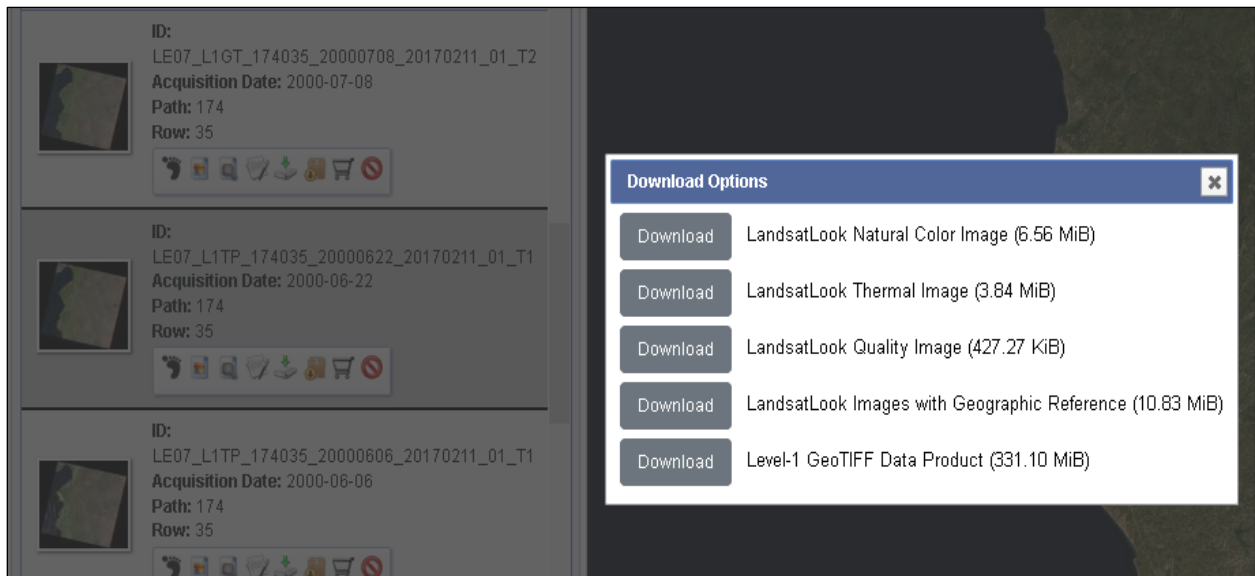


Figure (3- 2): Download Landsat 7 satellite image from USGS

Satellite	Sensor	Date	SLC (ON – OFF)
Landsat 7	ETM+	22/06/2000	ON
Landsat 7	ETM+	04/07/2010	OFF
Landsat 7	ETM+	12/05/2020	OFF

Table (3- 1): Downloaded satellite images for Land Use Land Cover change

### 3.1.1.2 Landsat 7 Scanline Failure:

After speaking about how to get the data, the last table mentioned Scan Line Correction (SLC), when it was turned on/off. This problem appeared because of the data of satellite images; the first image was captured before the failure in Landsat 7 ETM+ Scan Line Correction. The next two images were after the failure, which was happened on May 31, 2003. Satellite images of 2010 and 2020 were filled with black stripes (gabs). The data of these gabs were missing due to the permanent failure of the satellite. Figure 3-3 shows an example of the downloaded satellite image in 2020 with gabs (RGB = 4-3-2).

To fix this problem, gab-mask files that USGS offered after the failure were used in the project to fill out the black stripes with data. Indeed, this filling will not be perfect, because the data will be calculated from the neighbor cells by resampling using Inverse Distance Weighting (IDW), not by obtaining the exact data in these stripes. However, this is the only way to fill the gabs to getting good results with Landsat 7, and using gab-mask to fill image data is faraway better than making classification with ignoring black stripes.

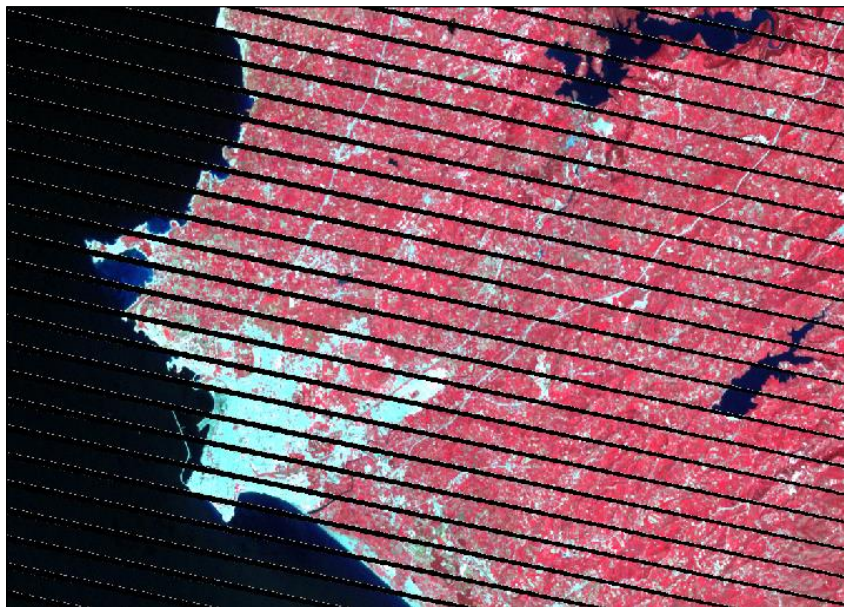


Figure (3- 3): ETM+ Scan Line Correction error in Latakia image (2020)

By using satellite image bands one by one, and using the GDAL tool (fill nodata) in Raster analysis, it will be easy to correct and fill the missing gabs using interpolation from other pixels values (figure 3-4 shows image after filling the gabs). The process is easy; just add each

band with its gab-mask file (TIF), and the result image bands will be in a good condition for the next calculations and processing steps.



Figure (3- 4): Latakia 2020 Landsat 7 image after filling nodata (gabs) values

### **3.1.2 Classification of satellite images:**

This process will be the way to find differences in classes between studied years. Classification process was done using Semi-Automation Classification plugin in QGIS. The most interesting part of this plugin is that it has almost all tools to finish classification, where tools are divided respectively to pre-processing, processing and post-processing.

#### **3.1.2.1 Pre-processing tools:**

First, the satellite image will cover more than the area we need to study. So, after setting the band that we want to work with in band set and applying Landsat 7 ETM+ in wavelength quick settings, the plugin has a pre-processing tool that allows the user to clip area of interest from each band in one click by clipping area according to coordinates, vector layer or simply drawing on the image. Saving clipped data in a separate folder is important in order to use it in the next step. The clipped area was Latakia with a part of the sea, because there is no satellite image for the southern part of Latakia in 2010 that forms the whole extent of Latakia when using the merge tool in QGIS.

The next step after clipping Latakia governorate is to get rid of reflectance on the image; here it is the assignment for atmospheric correction tool. In preprocessing tools, all satellites data

that Semi-Automation Classification plugin deals with are existing. As Landsat 7 satellite captured our images, we need to use Landsat and insert our clipped data with metadata file (MTL), which will be downloaded with image data files. Before running the process, activating applying atmospheric correction is the most important step. The results will be saved in atmospheric correction file (a new folder we created), where this file must be used for the next classification steps. Note that after each step of clipping and applying atmosphere correction, band set must be updated for new data. Therefore, we deleted the whole satellite images, and inserted clipped data (bands) instead, and then we deleted clipped data and used bands after finishing atmospheric correction.

The result of preprocessing tool is to get pure image data with our needed area to study, without reflectance, and with obtaining virtual raster that consists of all bands (Semi-Automation classification supports making it without using raster calculator). In this virtual raster, the user can choose three bands to show (RGB); this gives a better visualization to the determination of classes, because there are standard colors for each class, and how it has been visualized on satellite images after setting the appropriate RGB. Some examples for this are 3-2-1 bands for natural colors, 4-3-2 bands for infrared colors (vegetation), 5-4-1 bands for agriculture, 4-5-3 for land/water, etc... (Figure 3-5 shows bands after atmospheric correction in layers, and 4-3-2 bands for vegetation).

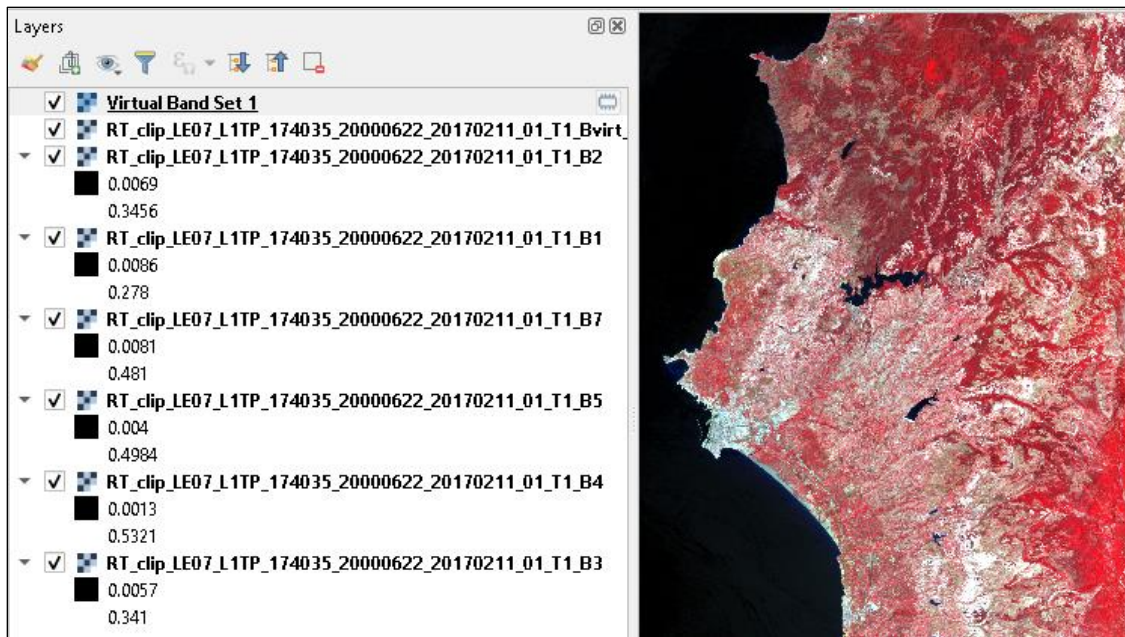


Figure (3- 5): Atmospheric correction bands and 4-3-2 virtual band set for Vegetation

### **3.1.2.2 Processing tools:**

Many steps are available here to finish the classification process; the first thing is the process has to be done with supervised classification. So, before moving to band processing in Semi-Automation classification plugin, there is an extension tool for the plugin, which can be added from panels, and it is called SCP Dock; it helps to take training data, calculating signatures and form classes in SCP training file.

#### **3.1.2.2.1 Training Inputs:**

Training inputs are vector polygons, which can be used to define many classes in satellite image. This will be done by taking similar training inputs for each class with the same color, and same features. As mentioned above about RGB, colors can be detected using suitable bands for each class to visualize class features well. From SCP Dock, a new training input file was generated for each satellite image (cannot use the same, because there will be differences from one image to another). After generating the file, there are four fields below the training data rectangle. On the left hand side, there are Micro Class ID (MC ID) and Class ID (C ID); here the user can create large classes, and insert some micro classes inside them (seas, rivers, lakes for water class). On the right, the user can write micro classes and classes names.

For our project, classes of (Water bodies, Agriculture, Forests, Buildings and Bare Soil) were taken, and after defining the number and name of each class, many training data polygons were chosen (figure 3-6) by clicking on creating a ROI polygon from SCP Dock tools until getting the best result for each class classification. After we finished creating training data for the class, signatures will be created for this class regardless of other classes, which will be calculated one by one after choosing training data for them. Training inputs file will be saved on computer, and the user can open it anytime in QGIS SCP Dock tool.

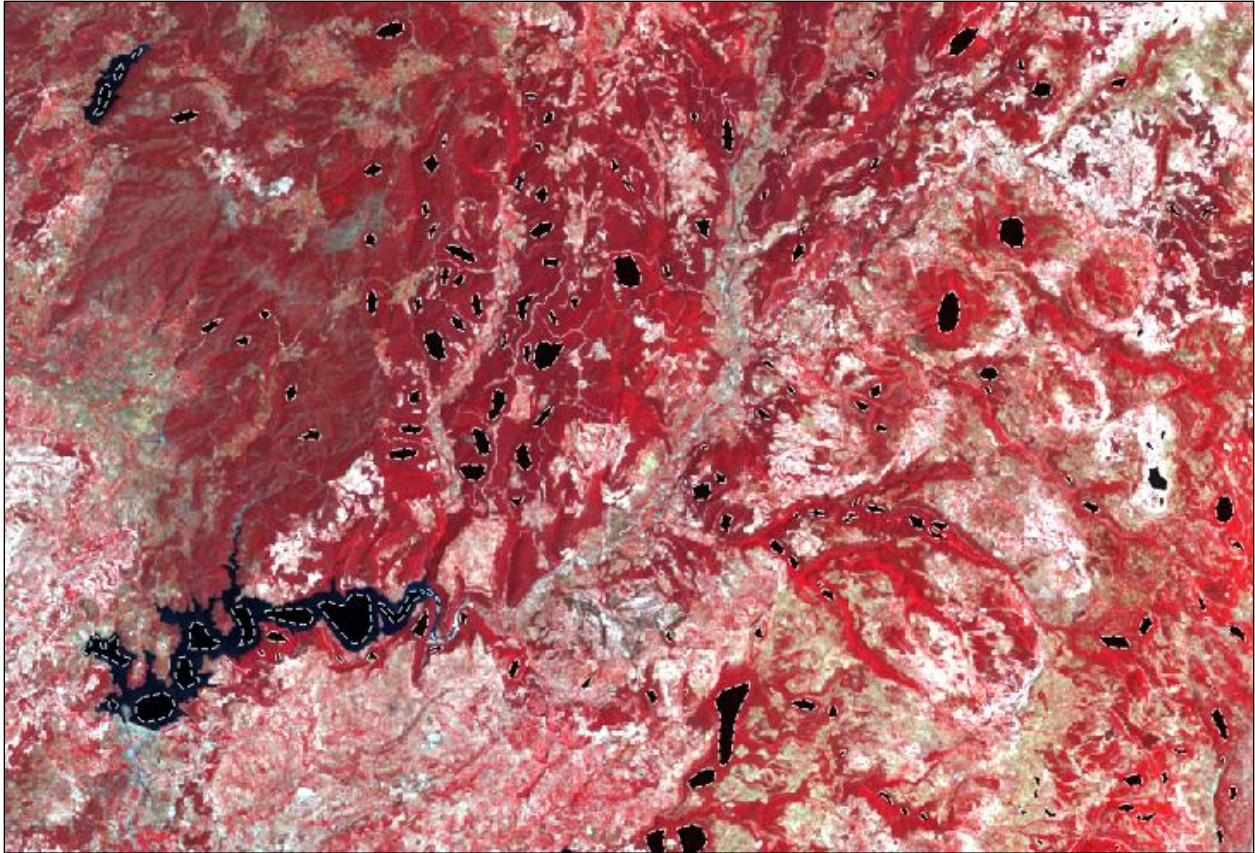


Figure (3- 6): Training Inputs on Landsat 7 satellite image of Latakia (2000)

#### **3.1.2.2.2 Classification Algorithm:**

After drawing sufficient training inputs, the next process is classifying satellite image to classes according to training inputs (classification tools can be found in band processing tools in Semi-Automation Classification plugin). The used algorithm was Maximum Likelihood, because even if it is more complicated than other algorithms, it gives better accuracy for classification. Simply, after choosing algorithm type and the class ID, click run. A classified satellite image will be generated, and the process of editing training data can be repeated if the results of the classification do not satisfy us (make the same process of taking new training data and applying classification for other satellite images). Classes colors are as follows: blue for water bodies, light green for agriculture, dark green for forests, grey for buildings and yellow for bare soil.

In 2010 image classification (not in other images), there were some clouds on the seaside. Therefore, they were processed in the classification like bare soil class (figure 3-7). However, this will not affect the important result of the classification and these areas were ignored.

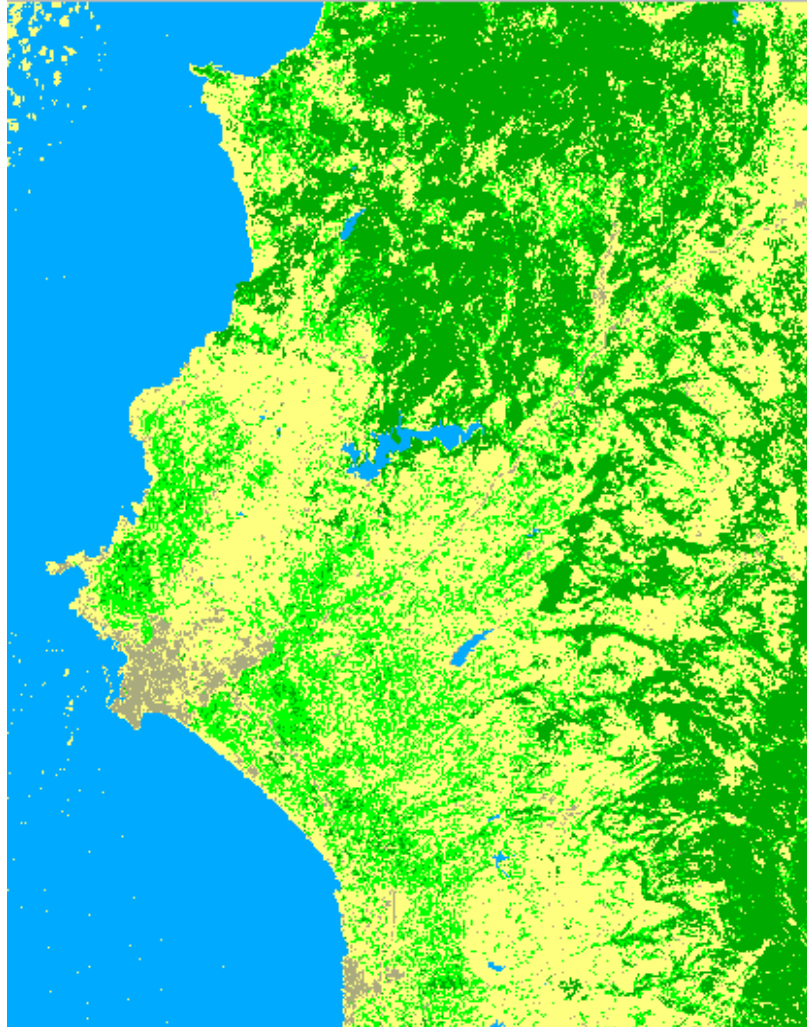


Figure (3- 7): 2010 classified image (Maximum likelihood classification)

### **3.1.2.3 Post-processing tools:**

#### **3.1.2.3.1 Accuracy assessment:**

Semi- Automation Classification plugin gives us a tool, which calculates the accuracy of our classification (it calculates accuracy for each raster cell using polygon control points). However, there is another tool in Orfeo toolbox for machine learning, which is specialized in accuracy calculating. It is called Compute Confusion Matrix. This matrix helps us get kappa index

with overall accuracy of results (it calculates accuracy by searching each cell center, and comparing these centers with vector control points/polygons that we take to calculate accuracy).

The second tool (ComputeConfusionMatrix) was used for this project. First, after creating a point vector layer and inserting the ID by class order among with generating another field, that defines each taken point for its class; one hundred control points were taken (20 for each class). Then, after inserting classified image, and ground truth vector point reference layer with defining its field name (class) in the tool window (figure 3-8), the result of the accuracy will be formed, and it can be saved as text file, where kappa index, overall accuracy and matrix accuracy values for each class will be represented (figure 3-9).

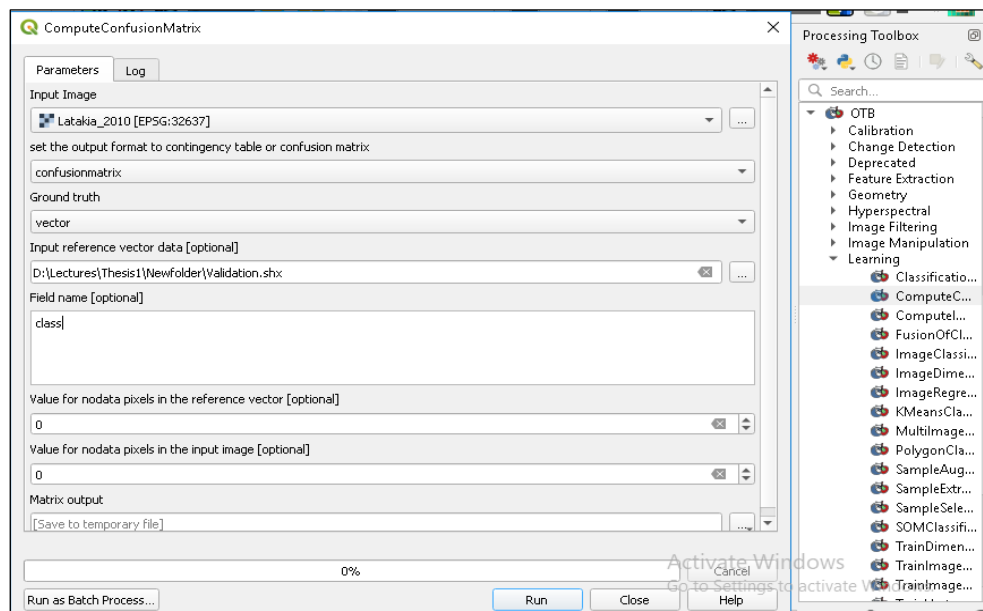


Figure (3- 8): Compute Confusion Matrix window in OTP toolbox (Learning)

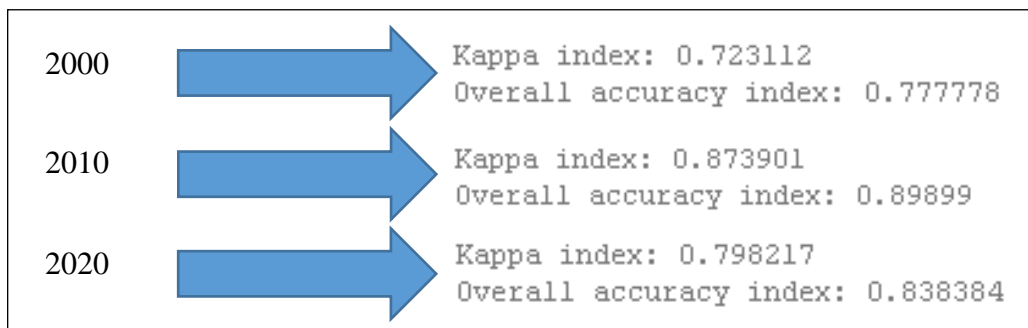


Figure (3- 9): Kappa index and accuracy values for each classified image

To be sure that the classification is ok, Kappa index must give a value above 0.5, and it will be better if it is above 0.6 (when this value approaches 1, the classification will be more accurate). The main diagonal of the matrix must have values above zero, and almost all other values will be zero. When all values are zero, this means that Kappa index is one, and this is impossible to happen for many classes. So, there must be values above zero, but it is recommended to get a few values like this, and they have to be near zero to get an accurate classification of the image. Otherwise, there will be a problem in the classification or vector control points, and then these steps must be recalculated.

### 3.1.2.3.2 Classes accuracy and area calculation:

By the way, regarding the accuracy for each class, this can be calculated and recognized from the confusion matrix, and each class will have a row of vector reference labels and column of produced labels in classification. Except the value of this class in the main diagonal, other values must be zero to get a perfect agreement for this class; but it is ok to get few values near zero without large numbers far above zero.

The overall accuracy can be computed easy and manually by getting the sum of values of each row and column in the confusion matrix, where the sum of columns values will equal the sum of rows values. In other words, when calculating the sum of all values in the confusion matrix including main diagonal, and then divide them by the sum of the main diagonal components values, the overall accuracy for the classification will be in hands. Here is the equation for the calculation of overall accuracy:

$$\text{Overall Accuracy} = \frac{\sum \text{main diagram components of the confusion matrix}}{\sum \text{all values in the confusion matrix including main diagram}}$$

Classes areas can be obtained from post-processing tool in Semi-Automation classification (Classification report). By adding the classified image, the user can get an Excel table contains all information about each class for many things (pixels number, areas, and percentage of areas will be generated).

### 3.1.2.3.3 Classes Changes Calculation:

The first main goal of this project is to visualize changes that happened to the studied area between 20 years. This process will come after the final classifications. To calculate changes, there is a tool in Semi-Automation classification in post-processing menu, and it is called Band calc. However, raster calculator in raster panel can do the same thing, and it is the main calculator in QGIS. The aim is to visualize all changes, which were deleted and added to classes year by year (2000-2010-2020).

After opening raster calculator, the change between two years is calculated for five classes and three years. This means that the process was repeated for 20 times to get all changes; the first ten times are for what was removed in year 2000, and what was added to year 2010 for each class; and the other ten are for the next ten calculations. Changes of class between two years has the same equation:

```
Removed from 2000 = "Latakia_2000@1" != "Latakia_2010@1" AND "Latakia_2000@1" = 3
```

```
Added to 2010 = "Latakia_2000@1" != "Latakia_2010@1" AND "Latakia_2010@1" = 3
```

These two equations are extracted from the project, and the meaning of the first equation conditions is letting the program calculates the third class (class ID) areas for year 2000, whereas this class is not existing anymore in this areas in 2010 (changed to another class type). The second equation will show what is added to this class in 2010, which was another class type in 2000.

The output layer of the calculation will be in single band grey color (black and white). The white color indicates changes in this class. It is better to change these colors for better visualization, and this is by changing the render type in symbology for Paletted/Unique values. The color of the added features to the class is blue, and the removed features are in red. Since the areas with no changes are not needed to display on the map, the black color (no change) sated to be 100% transparent (figures 3-10 and 3-11) show two of the project outputs about removed and added features respectively). This visualization makes it easy to understand the changes in the study area. The result layers are exported to rendered image in EPSG: 6871 – WGS 84 / Pseudo Mercator in

order to make them ready for the next and final step, which is visualizing these changes on web-based platform.

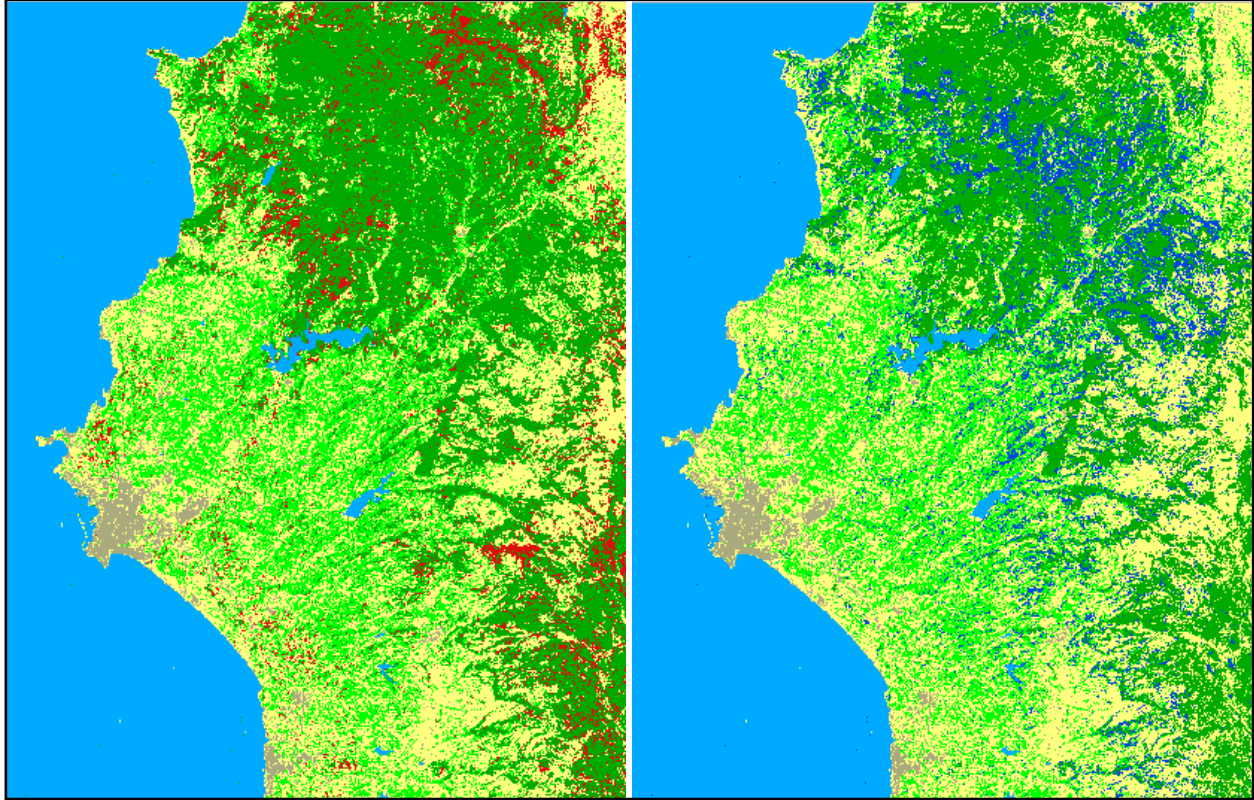


Figure (3- 11): Removed forests between 2010 and 2020      Figure (3- 10): Added forests between 2010 and 2020

## **3.2 Burn Severity (Fire Infection) section:**

### **3.2.1 Data Acquisition and preprocessing tools:**

The first step is to download four Landsat 8 images from USGS. Here, there is something different. Two nearby images were downloaded in the same date in order to merge them to expand the whole area of Latakia. This is important in burn severity, if satellite images are existing for the same date to know every affected area. The first two images were one month before the fire on 09/09/2020 (images after this date include clouds), and the other images were on 27/10/2020 after the fire terminated. A valuable thing is that Landsat 8 images do not have the same problem as

Landsat 7 in scan line error. Also, Landsat 8 has better characteristics and specifications than all previous versions.

Downloading process is the same for Landsat 7 images, except choosing Landsat 8 data set to represent available satellite images. After downloading images, they must be opened one by one in QGIS to do the subsequent operations on them.

Satellite	Sensor	Date	Region
Landsat 8	OLI, TIRS	09/09/2020	Latakia
Landsat 8	OLI, TIRS	09/09/2020	South Latakia
Landsat 8	OLI, TIRS	27/10/2020	Latakia
Landsat 8	OLI, TIRS	27/10/2020	South Latakia

Table (3- 2): Downloaded satellite images for Burn Severity map

After using merge algorithm in raster miscellaneous, inserting each two bands together and repeating this process many times, a new satellite merged images will appear. Figures 3-12 and 3-13 show the two merged satellite images, one before and the other after the fire.

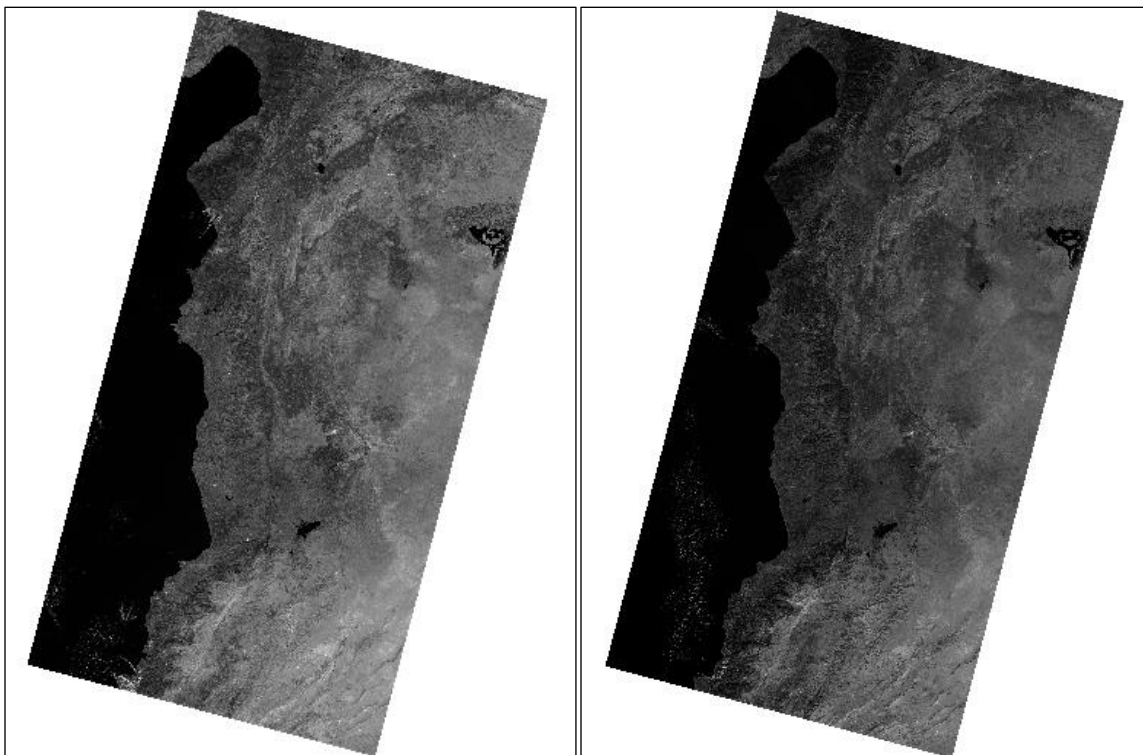


Figure (3- 12): two Merged images 27/10/2020

Figure (3- 13): two Merged images 09/09/2020

Regarding clipping, the used layer to clip Latakia extent was a downloaded file for Latakia governorate from Overpass-turbo website by typing boundary = administrative for Latakia, and this file was in JeoJSON format (Overpass-turbo website and the used code to choose Latakia are represented in figure 3-14). After that, Semi-Automation Classification has a feature that helps in clipping raster, the user can add vector layer, and clip the satellite image according to this vector.

Atmospheric correction must be done for these two images using clipped bands with metadata file. Clipping and Atmospheric correction steps will be after setting band set to Landsat 8 image bands. The final image after clipping and correcting is in figure 3-15 (for post-fire).

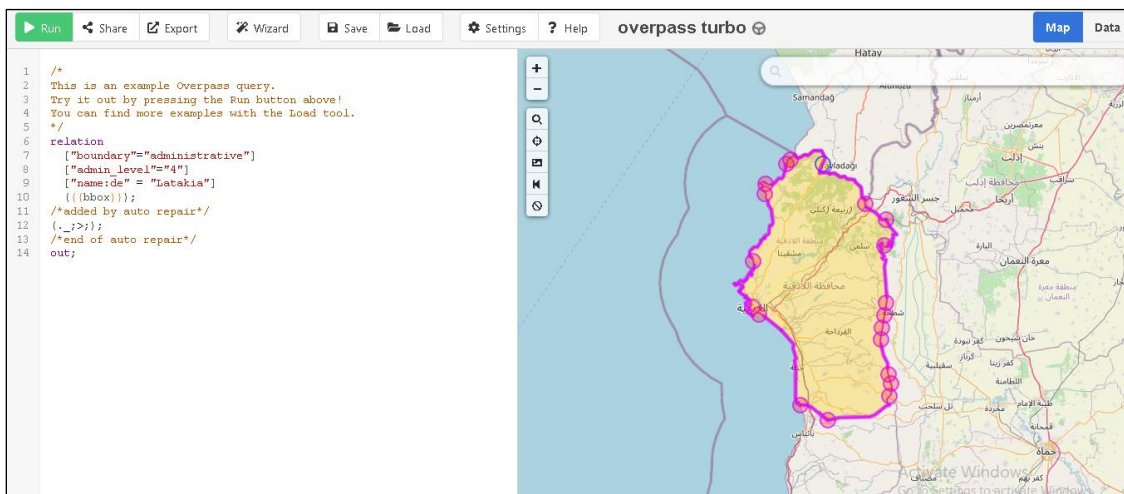


Figure (3- 14): Overpass-turbo user interface and code for downloading Latakia JeoJSON

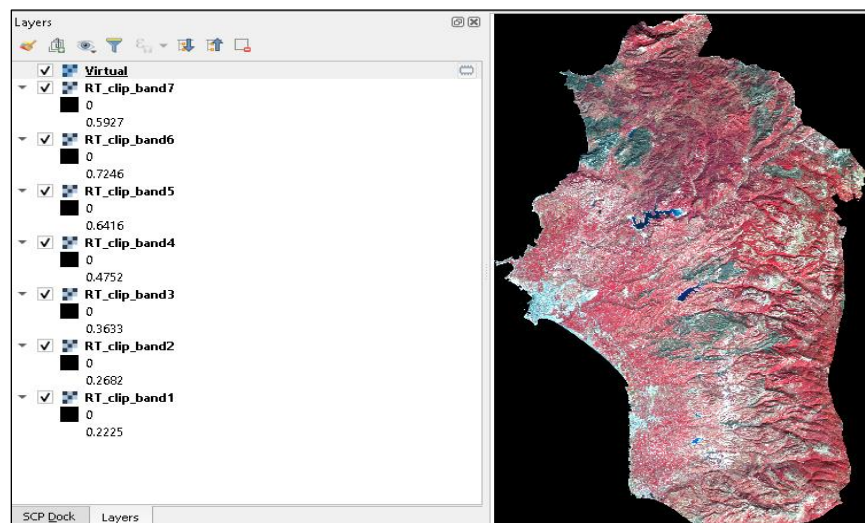


Figure (3- 15): Landsat 8 post-fire image after clipping and atmospheric correction

### 3.2.2 Normalized Burn Ratio (NBR) calculation:

NBR was calculated for both pictures, where just bands 5 (NIR) and 7 (SWIR) needed to be use in QGIS. By using the equation  $NBR = \frac{NIR-SWIR}{NIR+SWIR}$  in raster calculator, there was an access to get NBR images for both pre and post fire satellite images (figures 3-16 and 3-17).

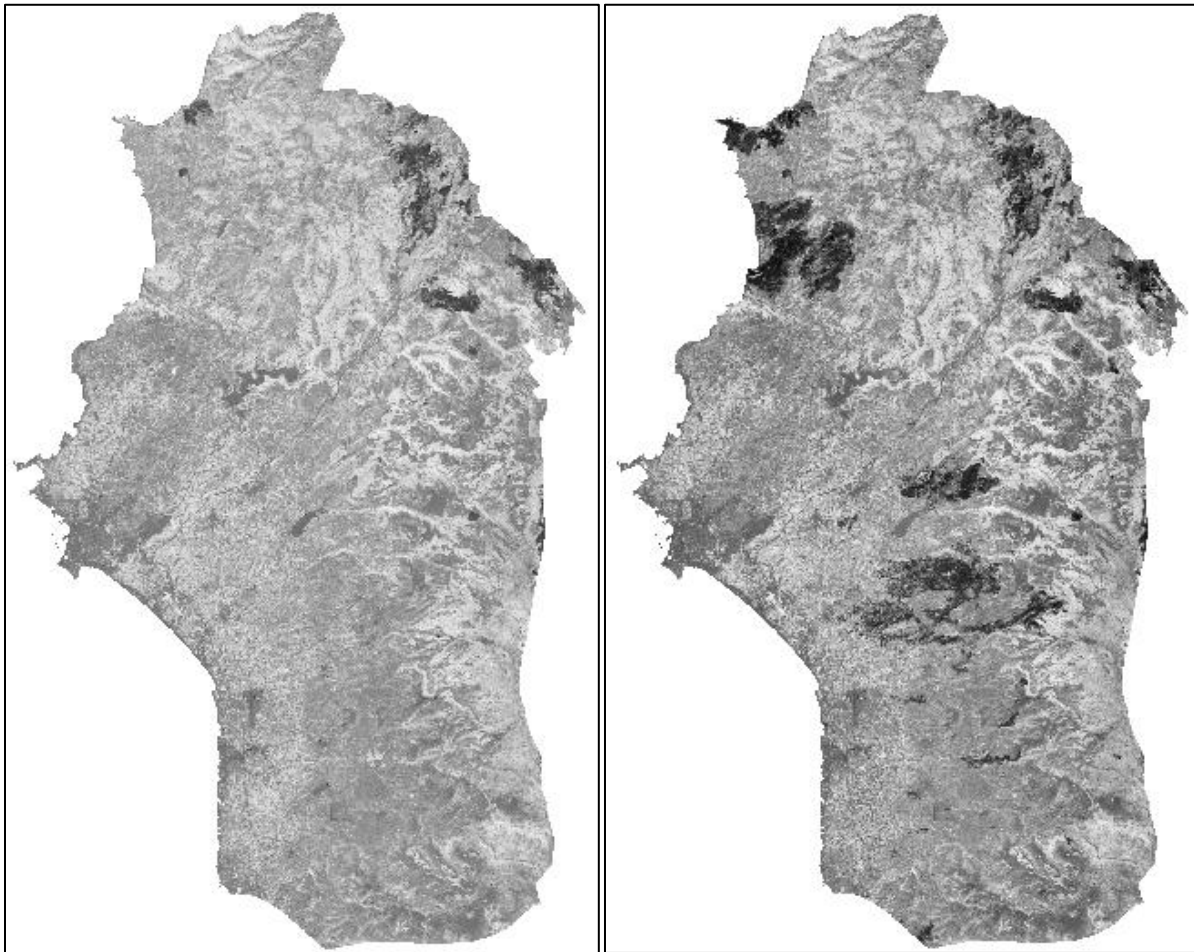


Figure (3- 16): NBR (pre- fire) image

Figure (3- 17): NBR (post- fire) image

### 3.2.3 Difference Normalized Burn Ratio (dNBR) calculation:

Evaluating NBR is not sufficient, even if some changes can be recognized when looking at these two NBR images. The result must be one image that includes areas affected by fires and ignores other normal areas. Here is the assignment for difference Normalized Burn Ratio (dNBR),

and it is calculated with subtracting post-fire NBR image from the pre-fire one ( $NBR = NBR(\text{Pre fire}) - NBR(\text{Post fire})$ ).

Here, the dNBR result will be in hands. By using symbology and colors for burn severity, areas can be modified with dNBR standard values after setting the render type for the image to single band pseudo-color. Figure 3-18 shows dNBR after calculating the last equation. This image is in single band grey render type as a default: grey indicates to fire areas, while white is normal areas without fires.

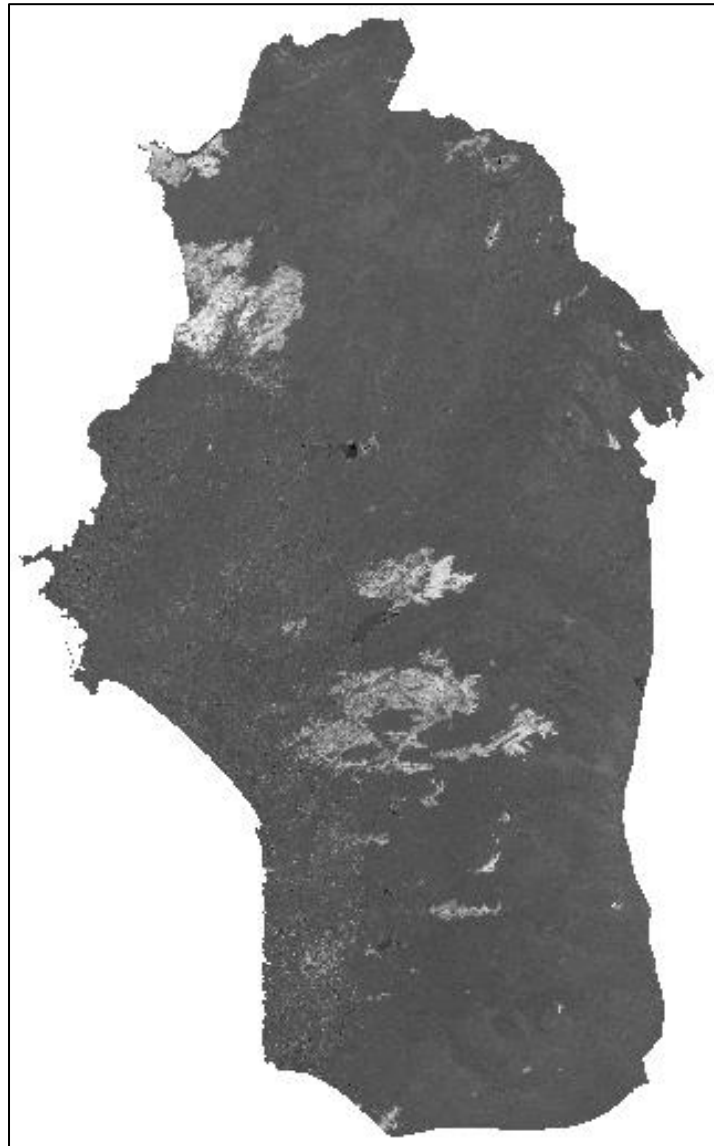


Figure (3- 18): dNBR result before changing symbology

## 3.3 Generating Web-Based pages:

### 3.3.1 Home page:

The last mission is checking the accuracy of the classification to be sure that it is perfect. The final use of QGIS program in this project is to provide showing the work on Web-based page on the internet using Notepad++ in codes generating. This step will help the audience around the world, who has some interests in remote sensing classification in general, and area of interest (Latakia) in particular to see the final results by clicking on URL to know what happened to this area during the years of study.

At first, it is important to have a home page represents basic ideas about the area of study and the importance of studying Land Use Land Cover (LULC) and Burn Severity (Fire Infections). The created home page was simple; three sections are embedded in this page. The first one is general information/introduction about Latakia; then LULC and Burn Severity definitions and the reasons to study them in this city; and the last section is about classes areas, accuracy assessment of LULC classification and Burn Severity levels areas.

Simple HTML and CSS tools were used to create the home page without using JavaScript, as the importance of JavaScript belongs to Web-Map page. Besides texts, some images about these paragraphs were added. CSS helped to get a good style according to titles, headers (h1, h2, h3) and normal sentences (<p>). In the second section, two links at the end of explanations lead to maps pages in one click (an example of designing a home page in HTML codes with choosing fonts and images classes that are defined in CSS codes is represented in figure 3-19).

```
<div id="main">
  <div class="inner">
    <header id="header">
      <a class="logo"><strong>Latakia (Syria):</strong> Change detection (Land Use Land Cover, and fire infection)</a>
    </header>
    <section id="banner">
      <div class="content">
        <header>
          <h2>Introduction:<br />
        </h2>
        </header>
        <p>- Latakia is a major Syrian city, which is situated in the coastline of Syria on the Mediterranean Sea in the west side of the country.</p>
        <p>- Three geographical zones divide Latakia, the first one is the Coastal Zone. This is the tinniest zone and the most important one.</p>
      </div>
      <span class="image object">
        
      </span>
    </section>
    <section>
      <header class="major">
        <h2>Aspects to study for change detection:</h2>
      </header>
      <h3>- Land Use Land Cover (LULC):</h3>
      <p><span class="image right"></span>Land Use Land Cover (LULC) has been the most important aspect to study for change detection.</p>
      <h3>- Fire Infection:</h3>
      <p><span class="image right"></span>Due to catastrophies that wild fires make, and for the reasons to study them in this city.</p>
    </section>
  </div>
</div>
```

Figure (3- 19): Example of HTML and CSS codes in generating homepage

### 3.3.2 Land Use Land Cover (LULC) and Burn Severity web-map:

Leaflet library helped us get the final map pages, two map pages were created (one for LULC, and one for Burn severity). These two web-map codes consist of Open street Map (OSM), and some of the same settings for both pages codes, due to using the same area with different satellite maps and another content visualization.

Largest data were in LULC map, like presenting layers of three kinds of classifications, adding change overlays that show added features (positive changes during the year) in blue color, and removed features (negative changes during the year) in red color for each class. One of the most interesting things is when moving mouse on any point of the page, the class type with its background color will appear as pop-up window for all three years (2000-2010-2020) in order to let the audience know what the class for this area was.

Fires map indicates all fire infections areas between two satellite images, which were taken in one month. Four types of severity are existing in this map in order to show low (yellow), moderate-low (orange), moderate-high (light red), and high (dark red) affected areas. Besides OSM, the background layer of a Bing Aerial satellite imagery is important to show a real image of the city before and after fire, where the user can activate fire overlay on this layer or OSM to visualize burned areas and their levels in the governorate.

For explaining some information about the usage of web-map code, here are some functions used in the creation process of web maps:

1. Leaflet library JavaScript call up using this function:

```
<script src = "leaflet/leaflet.js"></script>
```

2. A JavaScript file, which helps use an extension, and pick a color from a specified image without picking anything outside it.

```
<script src = "leaflet-imageoverlay-colorpicker.js"></script>
```

Here is an example of how to add image by taking its name and defining latitude and longitude for its boundaries to get its colors; the opacity is zero because we need to activate images for the process of color representing by mouse move. Boundaries are represented like [South-West],[North-East].

```
var one = L.imageOverlay.colorPicker('Image', [bounds]).addTo(map).setOpacity(0)
```

```
var two = L.imageOverlay.colorPicker('Image', [bounds]).addTo(map).setOpacity(0)
```

3. LayerGroup function: after defining a variable with this function, it helps include two images in one group. So, after activating this layer, two layers will be represented at the same time together (changes layers):

```
var group = L.layerGroup();
```

```
var one = L.imageOverlay('ChangeImage1',[bounds]).addTo(group);
```

```
var two = L.imageOverlay('ChangeImage2',[bounds]).addTo(group);
```

4. To insert layers and overlays into the map as layers window, the first thing is to define them in JavaScript codes, then add them to map as follows:

```
var layers={'firstlayer': one, 'secondlayer': two,}
```

```
var overlays={'firstoverlay': group}
```

```
L.control.layers(layers,overlays).addTo(map);
```

Layers button will appear on the upper right hand side, and it will consist of images layers and overlays (a small line between them) with names that were added to the last code (Layers: firstlayer, secondlayer / overlays: firstoverlay), where the user can active one layer, and more than one overlay if they exist.

5. To get the color for each class in order to use them in the legend and display them in mouse move on the image, RGB colors for these classes must be added:

```
var classes = { '0,170,255': 'first', '0,255,0': 'second', '0,170,0': 'third' }
```

6. The activation of mouse move and displaying years with colors and classes need many steps. First, define a variable for each image that is already activated (activated layers will display a pop-up window) and use ColorPicker extension inside it. Then insert another function, which is called getColor; this function picks RGBA (RGB with opacity) color exactly on the mouse position point. For the same sample:

```
let rgb0=one.getColor(e.latlng);
```

```
let rgb1=two.getColor(e.latlng);
```

Opacity is not needed in classes colors. So, by defining the first three values of RGBA with slice function, it is easy to get rid of the opacity:

```
rgb0=rgb0.slice(0,3);
```

```
rgb1=rgb1.slice(0,3);
```

The next process is calculating brightness for colors in order to choose font color depending on its value. The font color will be black, if the value is less than 0.35, and white otherwise (#000: black, #fff: white):

```
b=(rgb0[0]+rgb0[1]*2+rgb0[2])/1020;
```

```
let tc0=b>.35?'#000':'#fff';
```

```
b=(rgb1[0]+rgb1[1]*2+rgb1[2])/1020;
```

```
let tc1=b>.35?'#000':'#fff';
```

The last variable to define is to distinguish between colors for each class. It means that if one of the offered classes has one of the same colors as it exists in class RGB values, put the name of this class color.

```
let text0=classes.hasOwnProperty(rgb0)?classes[rgb0]:rgb0;
```

```
let text1=classes.hasOwnProperty(rgb1)?classes[rgb1]:rgb1;
```

To finish this process, pop-up window must be added to the map. With defining variables that were created, and adding style for the appearance of the window, the final pop-up window will be displayed after adding it to the map and removing opacity to the tooltip function:

```
content='2000: <span style="padding:5px;border-radius:5px;
```

```
background:rgb('+rgb0+');color:'+tc0+'"'>'+text0+'</span>
```

```
content='2010: <span style="padding:5px;border-radius:5px;
```

```
background:rgb('+rgb1+');color:'+tc1+'"'>'+text1+'</span>
```

```
tooltip=L.tooltip({opacity:1}).setLatLng(e.latlng).setContent(content).addTo(map);
```

7. Every map must have a legend, and this is what needs to be added as a final step in web-map section. Defining a legend has stable steps in JavaScript; the first thing is to determine its place on the map, then choosing an appropriate name of the map to put it inside the legend with the title of classes. After that, adding classes with colors and

styles using labels.push function, and finally determining that this legend refers to the HTML code before inserting it in the map.

```
var legend = L.control({position: 'bottomleft'});  
legend.onAdd = function(map){ var div = L.DomUtil.create('div', 'info legend');  
  labels = ['<h3>MapName h3><strong>Categories</strong>'];  
  for (var i in classes) {  
    labels.push('<i class="legendsample" style="background:rgb(' + i +  
    ')">&nbsp;</i> ' + classes[i]);}  
  div.innerHTML = labels.join('<br>').replace('<hr/><br>','<hr/>');  
  return div;}  
legend.addTo(map);
```

## **4. Results and Discussion:**

### **4.1 Overview:**

This chapter contains the whole results for two sections (Land Use Land Cover, Burn Severity). Regarding the first section, graphs, tables and figures will appear in this chapter with speaking about all five classes, and how they changed according to these 20 years. The second section will contain information and charts that represent the total damaged area, and burn severity classes areas in general. Nevertheless, percentages of these areas compared to Latakia governorate area are important to be calculated to determine if it is big or not before visualizing Latakia maps after classification. In other words, data charts indicate total areas per Km<sup>2</sup>, changes between them in the studied years or months, and data visualization for Latakia maps as the last result of the project. Last but not least, representing a web-based pages, that contain one home page with URLs that lead to final maps pages is the most important step in the project to show maps with layers and legends clearly for all interested people.

### **4.2 Land Use Land Cover:**

#### **4.2.1 Areas Calculation:**

According to reached results, information about areas in each land class in the studied years are obtained after finishing the final classification. This is important to represent changes of areas between years, and know how these classes increased or decreased in the face of other classes. This information will help imagine how these areas go, and expect what will happen in the future of these classes.

This can be obtained from classification report post-processing tools in Semi-Automation classification plugin, where the area of each class can be calculated for Paletted/Unique values symbology type. This tool helps get areas per m<sup>2</sup> for each class, and the user can change this unit easily to km<sup>2</sup> ( $\times 10^{-6}$ ). Figure 4-1 shows areas data after calculating them with classification report tool, and design them into chart using Excel.

Bare Soil has the most area size in all years, but it decreased a lot from 2000 to 2020, because it was replaced by agriculture and forest areas, which grew significantly during these years. Water Bodies are almost the same, with the exception of lakes, from which the water can

dry up at times due to lack of rain and other climatic reasons. 2010 image has less water than other years if you look at the statistics, but actually it is near their values and this lack is because of some clouds that presented as bare soil in the sea. The issue is that water bodies included sea, which is not on Latakia land, and their values are high because of that. Buildings areas rule in each country will be more year by year, because every year there are new buildings that replace other areas. Therefore, buildings were going increasingly from 2000 to 2020, but actually, the area of them is still small, and this is the default, because buildings are always the smallest parts of countries and cities in general.

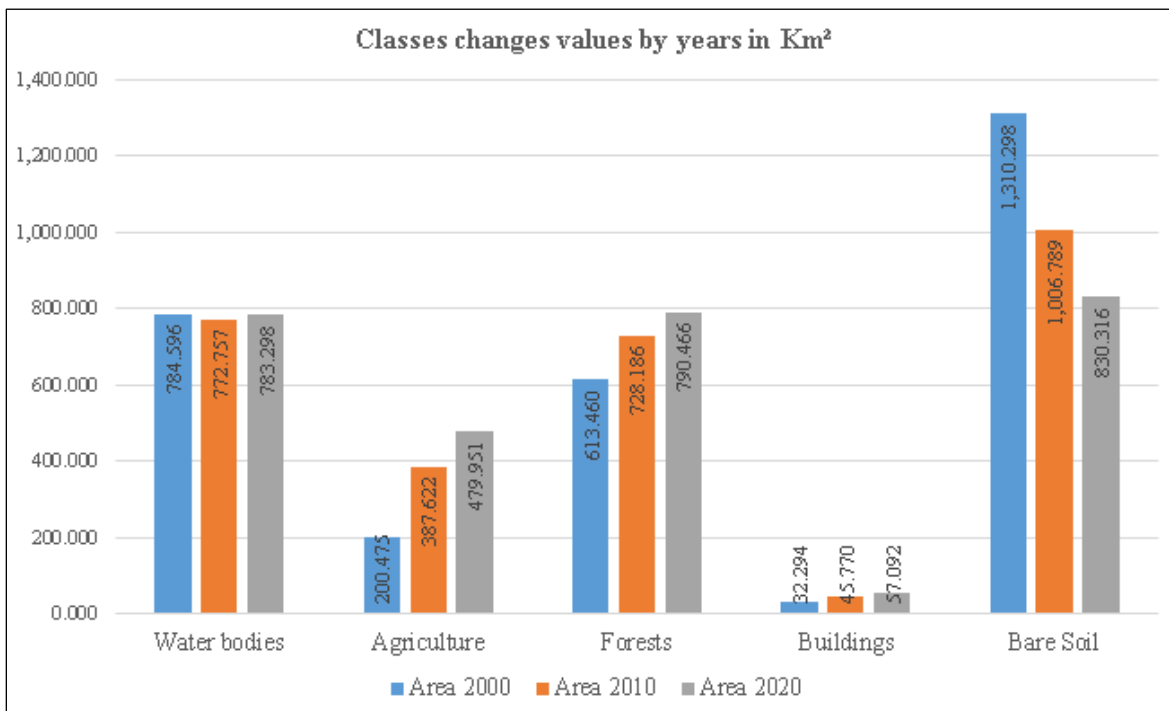


Figure (4- 1): Classes values chart in 2000-2010-2020

#### 4.2.2 Accuracy assessment tables:

In confusion matrix values each year, it is possible to deduce the best class after classification. This is by looking at the cells in the same row and column of the class, and dividing the main component of the diagram for this class by the sum of components in row and column including the main component. For example, to calculate the accuracy of forests in 2020, the number 20, which is the main component, will be divided by 27, because all other components are zero except 20 and 7, then the result will be 0.74 for this accuracy and so on.

In confusion matrix tables, the user can see the best class, which is definitely water bodies due to little changes of water, even if it takes large area of satellite image (these areas for water are almost constant because there will never be a change in the sea surface). Actually, water bodies is not the less important class in terms of classification studying. This is because the drying and filling of lakes appear in image changes and can be observed quickly. Below, there are three confusion matrix tables that show values with their Kappa Indexes and Overall Accuracy, where calculation of overall accuracy of classes separately and together is possible.

Class		Produced labels (Classification classes)				
		Water bodies	Agriculture	Forests	Buildings	Bare Soil
Reference Labels (Vector points)	Water bodies	18	0	0	0	1
	Agriculture	0	7	5	0	9
	Forest	0	0	20	0	0
	Buildings	0	1	0	13	6
	Bare Soil	0	0	0	0	19
<b>Kappa Index</b>		<b>0.72</b>				
<b>Overall Accuracy</b>		<b>0.78</b>				

Table (4- 1): Confusion Matrix table for 2000

Class		Produced labels (Classification classes)				
		Water bodies	Agriculture	Forests	Buildings	Bare Soil
Reference Labels (Vector points)	Water bodies	19	0	0	0	0
	Agriculture	0	11	4	0	6
	Forest	0	0	20	0	0
	Buildings	0	0	0	18	2
	Bare Soil	0	2	2	0	15
<b>Kappa Index</b>		<b>0.87</b>				
<b>Overall Accuracy</b>		<b>0.9</b>				

Table (4- 2): Confusion Matrix table for 2010

Class		Produced labels (Classification classes)				
		Water bodies	Agriculture	Forests	Buildings	Bare Soil
Reference Labels (Vector points)	Water bodies	19	0	0	0	1
	Agriculture	0	11	7	0	3
	Forest	0	0	20	0	0
	Buildings	0	0	0	20	0
	Bare Soil	0	0	0	0	19
Kappa Index		<b>0.80</b>				
Overall Accuracy		<b>0.84</b>				

Table (4- 3): Confusion Matrix table for 2020

Consequently, after calculating classes, the best class (except water bodies) is buildings. It has the highest accuracies for 2010, 2020 and comes after forests in 2000. While the worst class was agriculture, and this is normal due to the difficulty of distinguishing between forests (large areas), and agriculture (approximately the half forest areas each year). One issue is that, there is not a remarkable difference in satellite images between forests and agriculture in many areas, even when trying to use RGB band related to agriculture (4-3-2 or 5-4-1). Indeed, the most stable area all years was forests with less than 0.10 difference and very good accuracy between 0.7 and 0.8. Accuracy values can defer according to taken control points as reference data from google satellite map.

Accuracy change values factors can be a better classification, because there will be more correct control points on the ground with more accuracy. However, the accuracy of these classifications is the perfect one after many attempts to reach accurate classifications values, and these values will be way better, if the control points were polygons. Figure 4-2 shows values of accuracy for each class in the studied years, where recognizing the best class is easy from the best to the worst each year.

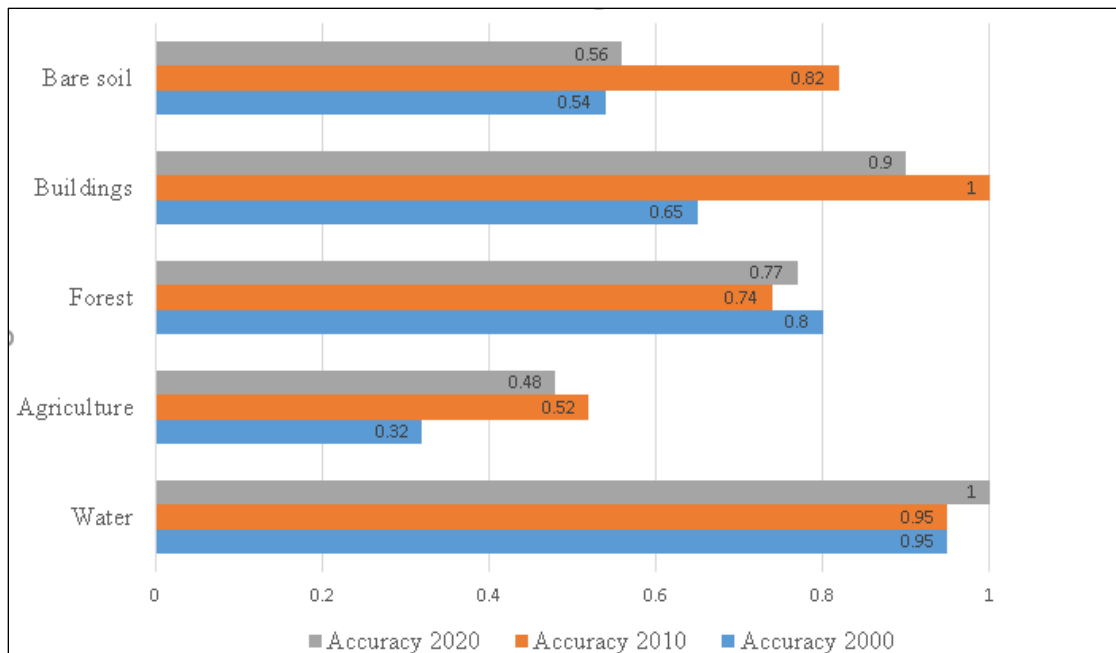


Figure (4- 2): Classes accuracy for the studied years

### 4.2.3 Final classified maps:

According to statistics above, data show that agriculture, forests and buildings are in growth during the last 20 years, while bare soil is decreasing, and this is better, because people will get benefits from agricultural lands and beautiful nature. Visualization of classes on maps is clear and easy to understand due to colors that are unique for each class. Figure 4-3, 4-4 and 4-5 in the next page show the final three classified satellite images with legends, where they have many differences between classes each year, and this can be recognized before seeing them clearly class by class after calculating changes.

The final step to finish working in remote sensing for LULC is to calculate changes for each class between two years. In this case, there will be 20 change layers; ten of them indicate removed features from the class (changed to another class), and the other ten are what was added to this class (changed from another class to this class). There are differences between changes according to areas, and this can be deducted from area changes, which were showed in figure 4-1 above. Figures from 4-6 to 4-10 show some calculated layers for each class changes between 2000 and 2010. The same thing in Figures from 4-11 to 4-15 between 2010 and 2020, where red shows which area was removed from the class, and blue is what was added to it.

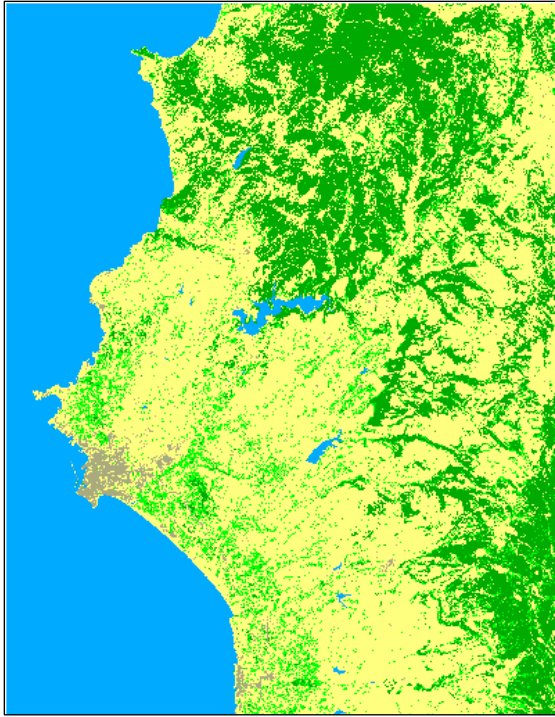


Figure (4- 3): Classification in 2000

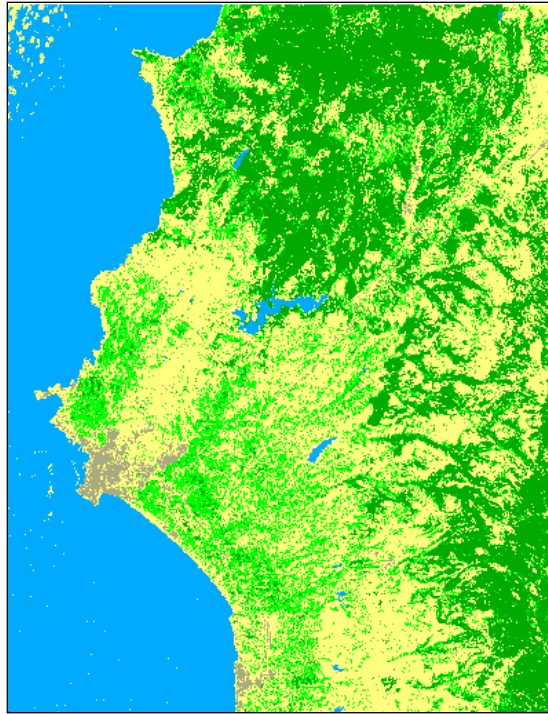


Figure (4- 5): Classification in 2000

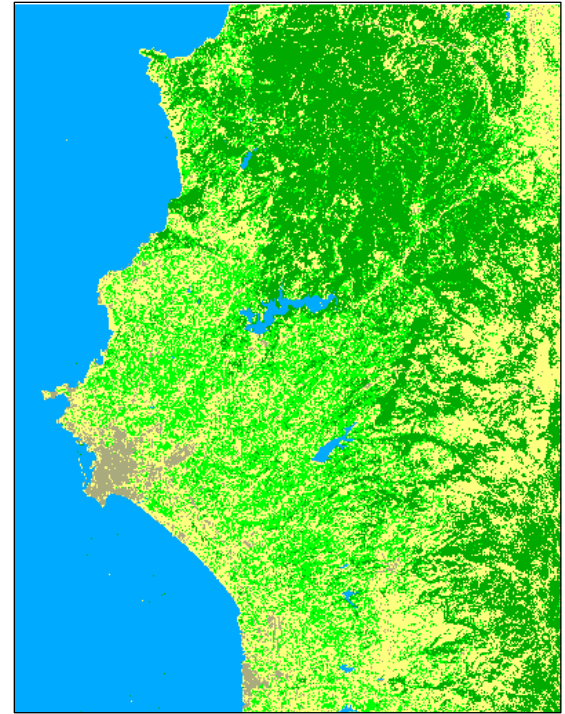
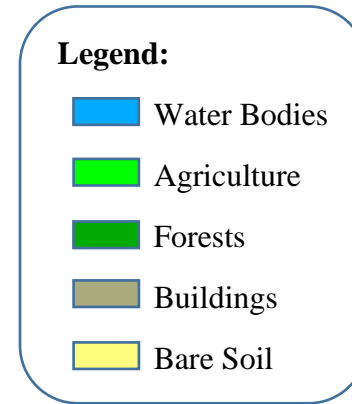
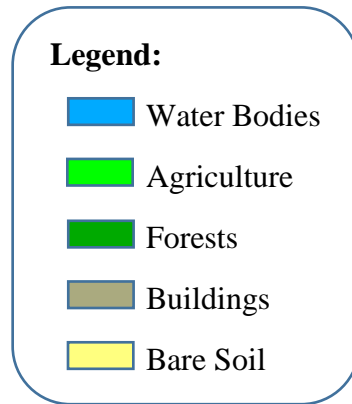
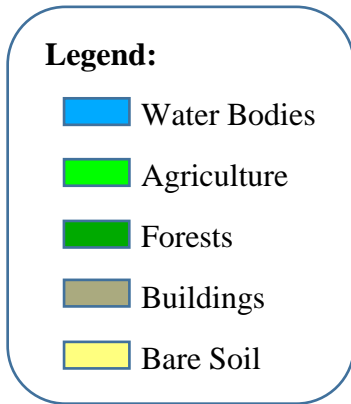


Figure (4- 4): Classification in 2000



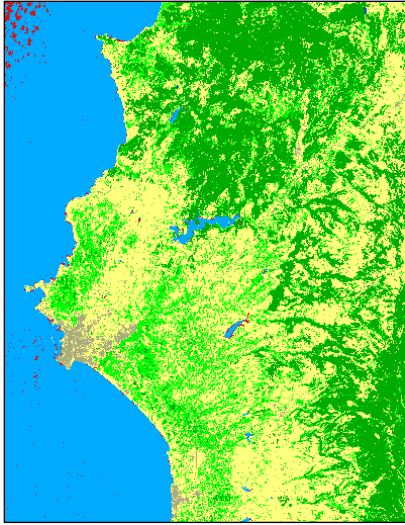


Figure (4- 8): Water bodies change 2000-2010

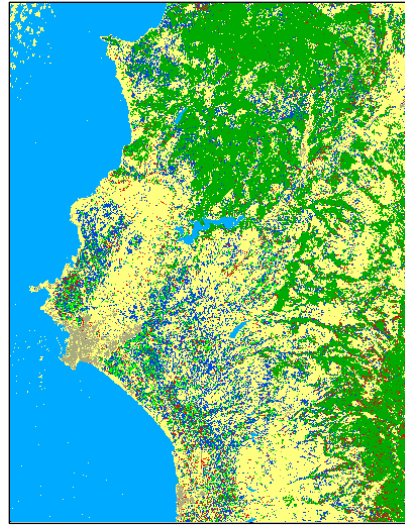


Figure (4- 7): Agriculture change 2000-2010

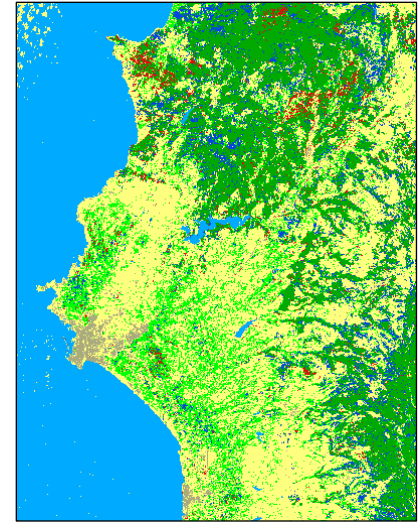


Figure (4- 6): Forests change 2000-2010

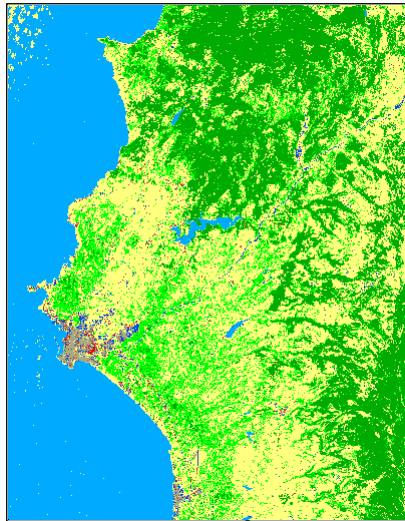


Figure (4- 9): Buildings change 2000-2010

**Legend:**

 Added Feature

 Removed Feature

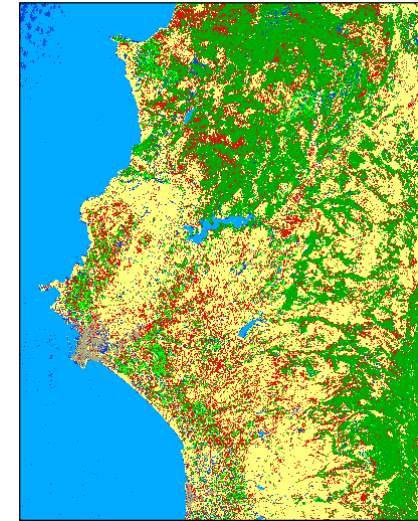


Figure (4- 10): Bare soil change 2000-2010



Figure (4- 13): Buildings change 2000-2010

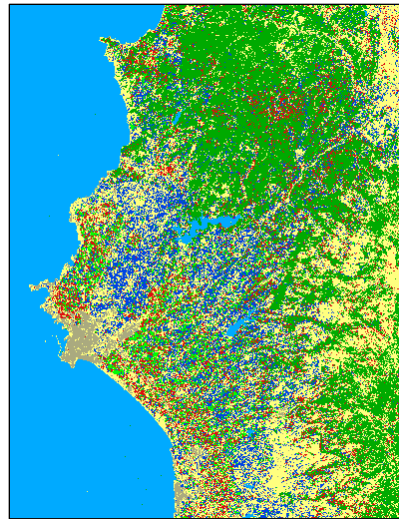


Figure (4- 11): Agriculture change 2010-2020

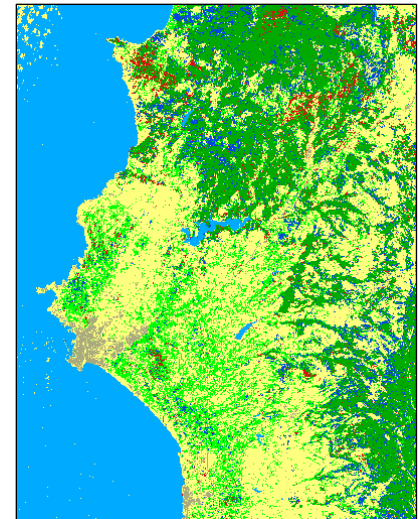


Figure (4- 12): Forests change 2010-2020

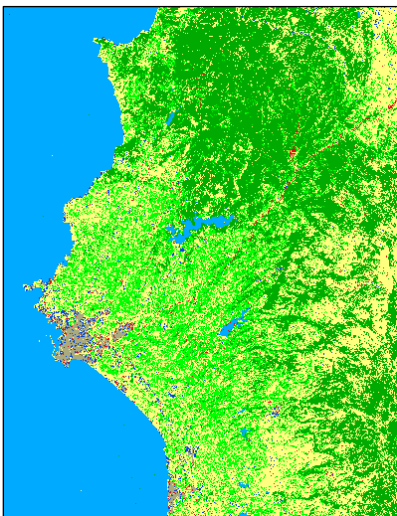


Figure (4- 15): Buildings change 2010-2020

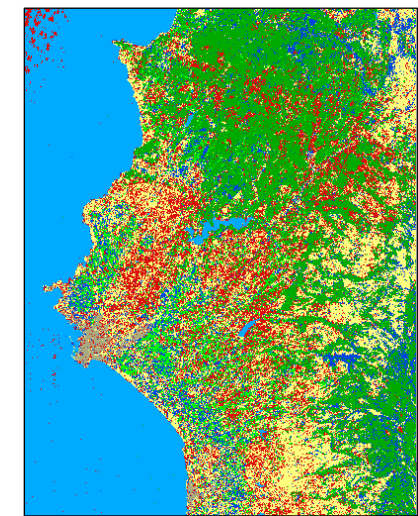
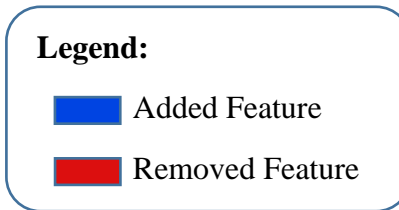


Figure (4- 14): Bare soil change 2000-2010

## 4.3 Burn Severity (Fire Infection):

### 4.3.1 Values and Colors:

The first result will not give details about the burn severity; it will just visualize burning areas with different white level colors. To show burn severity with difference Normalized Burn Ratio (dNBR) standard fires intensity values, the render type symbology will be set to Paletted/Unique values. The reason of choosing this render type instead of Singleband Pseudocolor is to let Classification report post-processing tool calculate the whole areas of burn severity level (between area ranges), while Singleband Pseudocolor will calculate each pixel area. After choosing Paletted/Unique values, the result will not be understandable, because ranges are not ok. Therefore, a processing toolbox in QGIS, which is called Reclassify by table, will help set ranges manually with chosen values from zero to four (Low to High severity) according to minimum and maximum values of each range. After setting fire intensity standard ranges (except 0.1 to 0.27 value because 0.20 to 0.27 gives better results), and changing colors according to burn severity colors, the dNBR map is ready to show fires in different levels of the studied area. Next figure 4-16 shows dNBR map after modifying symbology with main values and colors for burn severity.

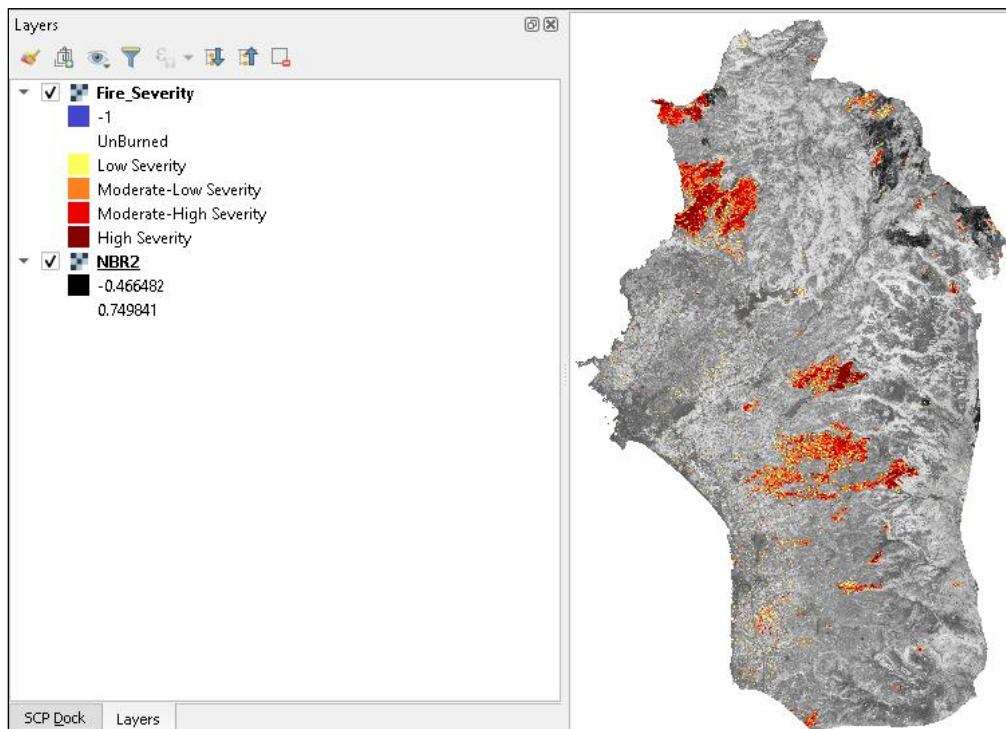


Figure (4- 16): difference Normalized Burn Ratio

### 4.3.2 Affected fires areas:

Calculating the areas of burn severity for each range is something very important. This calculation helps to know the affected areas, especially for this fire, which is considered the biggest one in Latakia history. As it is mentioned in information about Latakia, its area is between 2297 km<sup>2</sup> and 2437 km<sup>2</sup>, and the area of our map is around 2417 km<sup>2</sup> after combining unburned with burned areas. Moderate areas were bigger than low and high severity areas, while moderate-low was the biggest area with around 53.832 Km<sup>2</sup> (2.23%), moderate-high took the second place of 48.056 Km<sup>2</sup> (1.99%), low severity 29.254 Km<sup>2</sup> (1.21%), and high severity 27.077 (1.12%).

According to these values, the total fire area was around 158.217 Km<sup>2</sup> (6.55%). This is considered as a large part of a city in a few days. Unburned areas were about 2258.636 Km<sup>2</sup> (93.45%). Burn severity area values are in figure 4-17 (except the value of unburned areas).

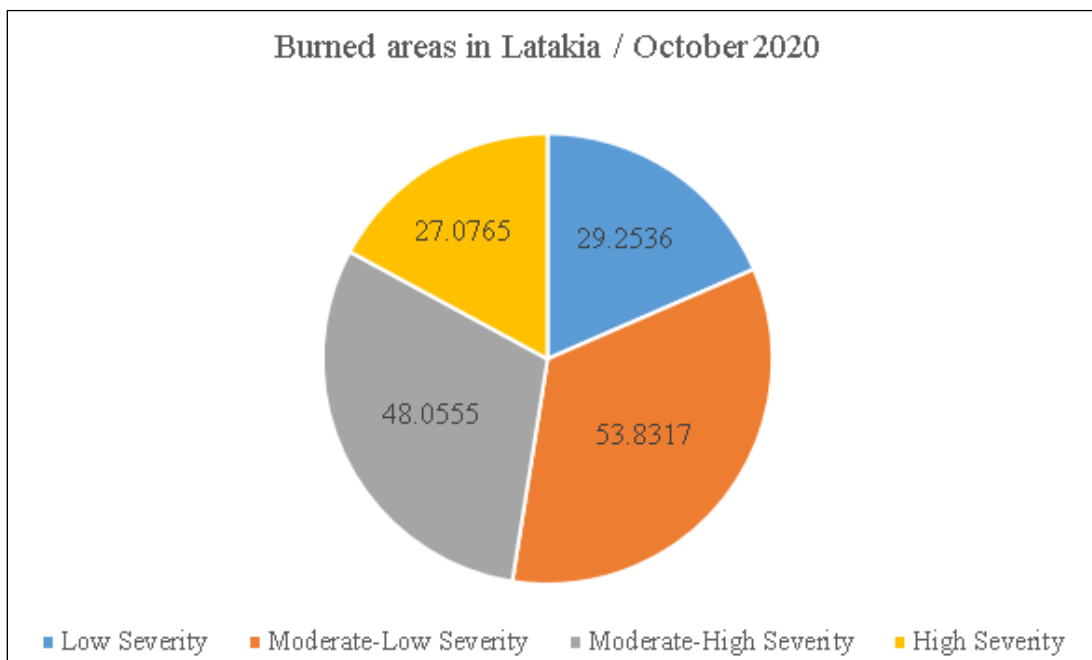


Figure (4- 17): Areas of Burn severity levels result

### 4.3.3 Final Burn Severity (Fire Infection) map:

Numeric values data are not sufficient to represent, if there is no data visualization. The final map shows burned areas locations in Latakia, where they were situated in the middle and north–west part of the country, with a few more areas in less fire spread. Burn severity levels are existing on the map with clear colors to help users understand the content of the map objects.

The background of these fires might be one of the resulted NBR satellite images, and both are accepted, because overlap fires will be above the image. So, pre and post fire NBR images will be the same in visualization (the important thing is to present Latakia). Burn severity map is in figure 4-18 below, where a legend of burn severity is near the map (unburned areas has 100% opacity).

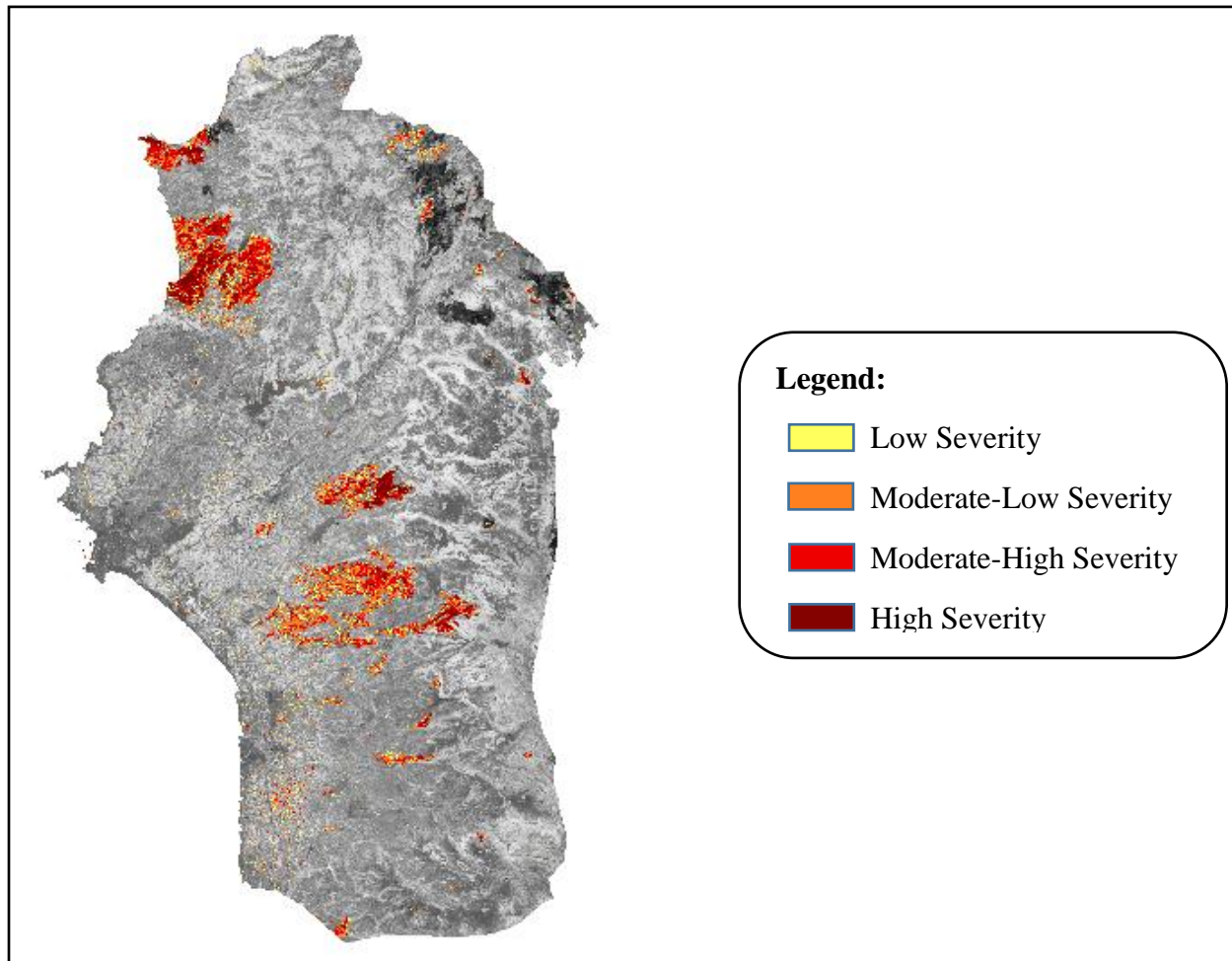


Figure (4- 18): Latakia Burn Severity map

## 4.4 Web-Based pages:

### 4.4.1 Home page:

The main purpose of the project is to add the final work in a web-based pages to show the created maps of LULC and Burn Severity. There were three pages related to each other by links. The main page that leads to map pages is the home page, where there are some general information about Latakia governorate, and a second paragraph of the studied sections in the project (LULC and Burn Severity). This paragraph contains two links, which lead to web-maps links. The home page also contains some numerical results about accuracy assessment for LULC, and areas calculations for LULC and burn severity as well, in order to prove to audience that this work is acceptable, and visualized data are in correct range. The first user interface after opening home page is in figure 4-19.



Figure (4- 19): Home page user interface

Link: [http://mercator.elte.hu/~mzv5w9/webgis/Thesis/Web\\_GIS/home.html](http://mercator.elte.hu/~mzv5w9/webgis/Thesis/Web_GIS/home.html)

### 4.4.2 Land Use Land Cover (LULC) Web Page:

The first important thing is calling up leaflet library. Bing Aerial map is the best choice to show real ground visualization on the map, especially if this map was talking about changes in

Land Use and Land cover. It helps the user to get a first look before checking classes and changes between years. Each classification was added as a switched layer to choose one by one according to which year to show. Overlap layers are below switched layers and the user can choose from them freely to see changes in each class. Moving mouse over the map shows what that class was in each year. The legend consists of two main categories, the first one is the colors of classes in classification, and the second is about added and removed features from each class. The design of this map (figure 4-20) with JavaScript functions made it easy to distinguish between classes from many directions (Layer and overlaps change, legend elements, mouse move above map, etc...).

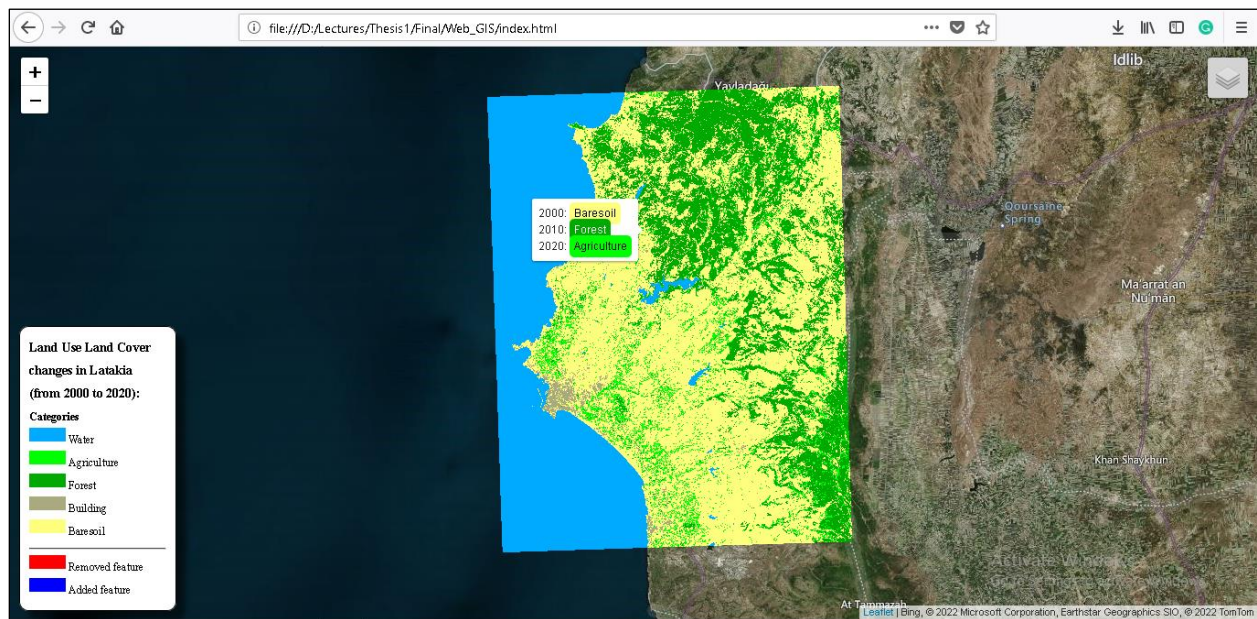


Figure (4- 20): Land Use Land Cover (LULC) web page

Link: [http://mercator.elte.hu/~mzv5w9/webgis/Thesis/Web\\_GIS/index.html](http://mercator.elte.hu/~mzv5w9/webgis/Thesis/Web_GIS/index.html)

#### 4.4.3 Fires Infection (Burn Severity) Web Page:

According to Burn Severity map, it is important to show fire spread in Latakia in order to show areas that were affected by this fire, whether it was a large or a small area. By the way, This map does not contain any satellite image background; it contains only the difference Normalized Burn Ratio, with 100% opacity for unburned areas. That is because the importance is to show burned areas on this map. Switched layers are OpenStreetMap, and Bing aerial to set one as a base map in the page, while overlap layer was only dNBR, which will show burned areas in different severities that are illustrated in the legend of the map (figure 4-21).

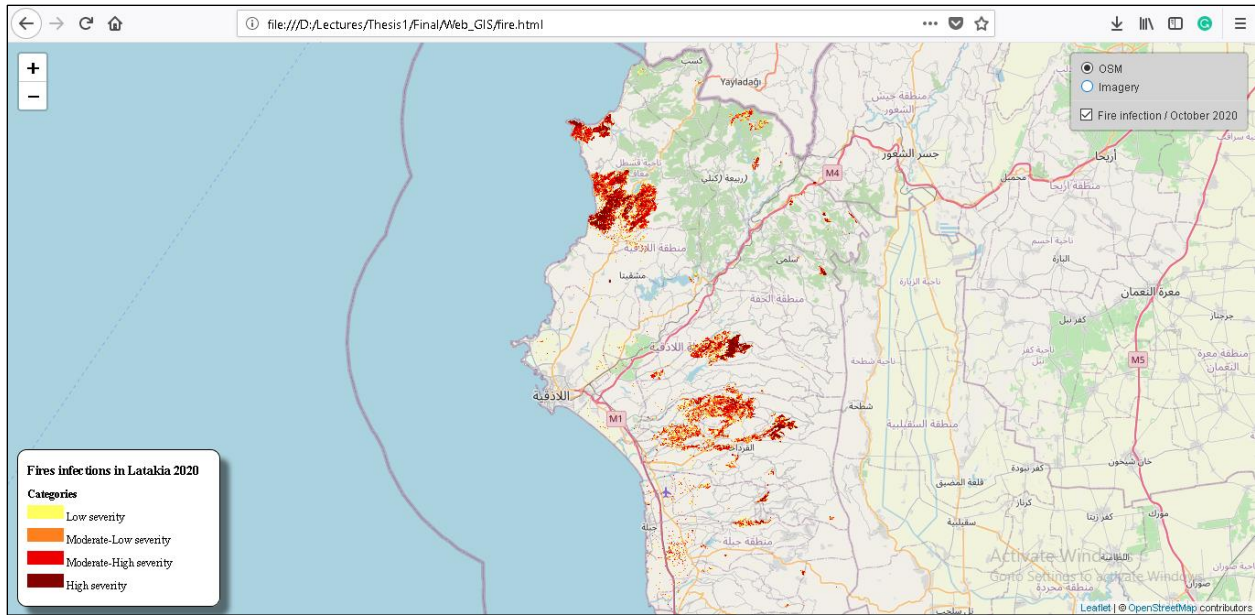


Figure (4- 21): Burn Severity (Fire Infection) web page

Link: [http://mercator.elte.hu/~mzv5w9/webgis/Thesis/Web\\_GIS/fire.html](http://mercator.elte.hu/~mzv5w9/webgis/Thesis/Web_GIS/fire.html)

## 4.5 Conclusion:

Many changes appeared to Land Use Land Cover in Latakia during the past 20 years, and this assumed to go increasingly in the future due to its location, and war effects. For example, agriculture is growing from a year to another. This relates to the lack of exports and economy, and people need to depend on their own to survive by investing the agricultural sector. Another positive thing is that forests are formed at the expense of Bare Soil. While buildings are increasing slowly as normal in each region. However, all these data were calculated and represented in the project in order to make it easy to know the differences for each class between years. Sharing these data on web pages is the essential part to show changes to people in values and maps visualization.

The detection of fire areas in the meantime of fire spread is the most important part to reduce the risk of fires. This will help to know the exact locations of fires and help the government to terminate it. Especially, Difference Normalized Burn Ratio (dNBR) presents burn severity areas, where this can be used to guess the extent of fires in the future. In addition, it is important to document previous fires using satellite images with areas and percentage of burning lands in order to help in revegetate and fix them as soon as possible. Web maps for burn severity is the easiest

way to visualize burning areas with fire levels, and this dNBR result map shows the largest area burned between few days in the whole history of Latakia.

Last but not least, Remote sensing change detection is the effective way to understand what is happening in small areas like streets, and big areas like cities, countries or even continents in many cases. In the hope that, this study will help give valuable information for those people, who want to get benefits to plan for the future with making decisions, and others who are interested to continue these studies in the upcoming years for the same or another region.

## References:

- Acharya T.D. & Yang I., (May, 2015). Exploring Landsat 8, *Properties*. . Retrieved at 03.04.2022, from:  
[https://www.researchgate.net/publication/311901147\\_Exploring\\_Landsat\\_8/link/589c0de6458515e5f4549e58/download](https://www.researchgate.net/publication/311901147_Exploring_Landsat_8/link/589c0de6458515e5f4549e58/download)
- Afram A., (October 10, 2020). New fires in Syria's coast countryside, *Eastern countryside of Latakia*. Retrieved at 02.04.2022, from: <https://npasyria.com/en/48005/>
- Al-doski J. & Mansori S.B & Shafri H.Z.M (November 10, 2013). Image Classification in Remote Sensing, pp.142-143, *Image Classification Techniques*. Retrieved at 18.03.2022, from: <https://core.ac.uk/download/pdf/234663192.pdf>
- Asokan A., Anitha J., (March 08, 2019). Change detection techniques for remote sensing applications: a survey, *Fig. 1*. Retrieved at 04.04.2022, from:  
<https://link.springer.com/article/10.1007/s12145-019-00380-5#citeas>
- Britannica, (July 26, 1999). Syria (Al-Jumhūrīyah al-‘Arabīyah as-Sūrīyah, Sūrīyah, Syrian Arab Republic), *Land, Relief*. Retrieved at 04.03.2022, from:  
<https://www.britannica.com/place/Syria#ref29929>
- Chabaan F. & Ali A. & Mohamed A., (July 23, 2020). Evaluation of the Accuracy of supervised and unsupervised Classification Methods for Landsat 8 Image Study Area: Tartous City. *Results of Classification*. Retrieved at 18.03.2022, from:  
[https://www.researchgate.net/publication/344462002\\_tqyym\\_dqt\\_trq\\_altsnyf\\_almraqab\\_wghyr\\_almraqab\\_lmryyt\\_landsat\\_8\\_mntqt\\_aldrast\\_mdynt\\_trtws\\_Evaluation\\_of\\_the\\_Accuracy\\_of\\_Supervised\\_and\\_Unsupervised\\_Classification\\_Methods\\_for\\_Landsat\\_8\\_Image\\_Study\\_Area](https://www.researchgate.net/publication/344462002_tqyym_dqt_trq_altsnyf_almraqab_wghyr_almraqab_lmryyt_landsat_8_mntqt_aldrast_mdynt_trtws_Evaluation_of_the_Accuracy_of_Supervised_and_Unsupervised_Classification_Methods_for_Landsat_8_Image_Study_Area)
- Cocke A.E, Fulé P.Z. Crouse J.E., (June, 2005). Comparison of burn severity assessments using Differenced Normalized Burn Ratio and ground data, *Abstract*. Retrieved at 11.04.2022, from:  
[https://www.researchgate.net/publication/228640487\\_Comparison\\_of\\_burn\\_severity\\_ass](https://www.researchgate.net/publication/228640487_Comparison_of_burn_severity_ass)

[essment using Differenced Normalized Burn Ratio and ground data/link/0912f50b4dcd42d07c000000/download](https://www.theoj.org/joss-papers/joss.03172/10.21105.joss.03172.pdf)

Congedo L., (August 27, 2021). Semi-Automatic Classification Plugin: A Python tool for the download and processing of remote sensing images in QGIS, *Summary, Statement of need, Overview of the Semi-Automatic Classification Plugin, pp1-3*. Retrieved at 20.03.2022, from: <https://www.theoj.org/joss-papers/joss.03172/10.21105.joss.03172.pdf>

Dempsey C., (March 16, 2021). GIS LOUNGE. *What is GIS?*, Retrieved at 13.03.2022, from: <https://www.gislounge.com/what-is-gis/>

D-maps, (2022). boundaries, hydrography, main cities, roads, names, *Map Latakia (Syria)*. Retrieved at 05.03.2022, from: [https://d-maps.com/carte.php?num\\_car=279420&lang=en](https://d-maps.com/carte.php?num_car=279420&lang=en)

Earth Observing System (EOS), (2012). *Landsat 7*. Retrieved at 07.03.2022, from: <https://eos.com/find-satellite/landsat-7/>

Elkhrachy I., (June 30, 2015). Flash Flood Hazard Mapping using Satellite Images and GIS Tools: A case study of Najran city, Kingdom of Saudi Arabia (KSA), *Confusion matrix and overall accuracy and Kappa coefficient for unsupervised classification process, pp10*. Retrieved at 23.03.2022, from: <https://www.researchgate.net/publication/279526150>

International Federation of Red Cross And Red Crescent Societies (IFRC), (October 23, 2020). Syria: Wildfires Emergency Plan of Action (EPoA) DREF Operation n° MDRSY005, *Description of the disaster*. Retrieved at 02.04.2022, from: <https://reliefweb.int/report/syrian-arab-republic/syria-wildfires-emergency-plan-action-epoa-dref-operation-n-mdrsy005-23>

Jolaiya E., (December 28, 2020). GIS LOUNGE, *WebGIS Section 3: Architecture, What is a Client/Server Architecture?*. Retrieved at 03.05.2022, from: <https://www.gislounge.com/webgis-section-3-architecture/>

Kiddle Encyclopedia (March 20, 2022). Latakia Governorate facts for kids, *Latakia governorate, Geography*. Retrieved at 06.03.2022, from: [https://kids.kiddle.co/Latakia\\_Governorate](https://kids.kiddle.co/Latakia_Governorate)

- Knight E. J. & Kvaran G., (October 24, 2014). Landsat-8 Operational Land Imager Design, Characterization and Performance, *Landsat-8 History* . Retrieved at 03.04.2022, from: <https://www.mdpi.com/2072-4292/6/11/10286>
- Mohamed N. & Mobarak B.(2016). American Scientific Research Journal for Engineering, Technology, and Sciences (ASRJETS), Change Detection Techniques using Optical Remote Sensing: A Survey, *Data used in change detection, Change detection steps* . Retrieved at 16.03.2022, from: <https://core.ac.uk/download/pdf/235049843.pdf>
- NASA, (April 8, 2022). Remote Sensing: An Overview, *Sensors* . Retrieved at 04.04.2022, from: <https://earthdata.nasa.gov/learn/backgrounders/remote-sensing#sensors>
- NASA, (December 5, 2019). Landsat science, *Landsat7, The Enhanced Thematic Mapper Plus (ETM+)*. Retrieved at 07.3.2022, from: <https://landsat.gsfc.nasa.gov/the-enhanced-thematic-mapper-plus-etm/>
- NASA, (March, 1999). Science Writers' Guide to Landsat 7 p3, *A New Era of Landsat Technology*. Retrieved at 07.3.2022, from: [https://eosps.gsfc.nasa.gov/sites/default/files/publications/1999\\_Landsat7\\_writer\\_guide.pdf](https://eosps.gsfc.nasa.gov/sites/default/files/publications/1999_Landsat7_writer_guide.pdf)
- NASA, (November 27, 2019). Landsat science, *Landsat 8*. Retrieved at 06.04.2022, from: <https://landsat.gsfc.nasa.gov/satellites/landsat-8/>
- NOAA, (February 26, 2021). *What is remote sensing?*. Retrieved at 14.03.2022, from: <https://oceanservice.noaa.gov/facts/remotesensing.html>
- Orfeo Toolbox, (April 27, 2022). Open Source processing of remote sensing images, *Orfeo ToolBox (OTB)*. Retrieved at 22.03.2022, from: <https://www.orfeo-toolbox.org/>
- OTB CookBook, (April 27, 2022). ComputeConfusionMatrix., *Description*. Retrieved at 22.03.2022, from: [https://www.orfeo-toolbox.org/CookBook/Applications/app\\_ComputeConfusionMatrix.html](https://www.orfeo-toolbox.org/CookBook/Applications/app_ComputeConfusionMatrix.html)
- Panuju D. R. & Paull D. J. & Griffin A. L., (June 1, 2020). *Change Detection Techniques Based on Multispectral Images for Investigating Land Cover Dynamics*. Retrieved at

- 15.03.2022, from: <https://www.mdpi.com/2072-4292/12/11/1781/htm#B1-remotesensing-12-01781>
- Pettinari M.L, Chuvieco E., Padilla M., Storm T., (December 30, 2016). ECV Fire Disturbance: Fire\_cci Phase 2, *Landsat-8*. Retrieved at 06.04.2022, from: [https://www.researchgate.net/publication/315519144\\_ESA\\_CCI\\_ECV\\_Fire\\_Disturbance\\_D14\\_Data\\_Access\\_Requirement\\_Document\\_version\\_23/link/58d39432aca2723c0a7791cb/download](https://www.researchgate.net/publication/315519144_ESA_CCI_ECV_Fire_Disturbance_D14_Data_Access_Requirement_Document_version_23/link/58d39432aca2723c0a7791cb/download)
- Richards J.A. (1986), Springer, Berlin, Heidelberg. Remote Sensing Digital Image Analysis, pp.173-195, *Supervised Classification Techniques*. Retrieved at 17.03.2022, from: [https://doi.org/10.1007/978-3-662-02462-1\\_8](https://doi.org/10.1007/978-3-662-02462-1_8)
- Singh A., (July 8, 2010). Digital change detection techniques using remotely-sensed data, *Introduction*. Retrieved at 15.03.2022, from: <https://www.tandfonline.com/doi/pdf/10.1080/01431168908903939?needAccess=true>
- Stevens J. & Smith J.M & Bianchetti R.A, (2012), Mapping Our Changing World, *Feature Versus Attributes*. Retrieved at 13.03.2022, from: <https://www.e-education.psu.edu/geog160/node/1930>
- Storey J. & Scaramuzza P. & Schmidt G. & Barsi J., (October 23-27, 2005). *LANDSAT 7 SCAN LINE CORRECTOR-OFF GAP-FILLED PRODUCT DEVELOPMENT*. Retrieved at 11.03.2022, from: [http://www.asprs.org/a/publications/proceedings/pecora16/Storey\\_J.pdf](http://www.asprs.org/a/publications/proceedings/pecora16/Storey_J.pdf)
- Swift J. & Goldberg D., (2019). The Geographic Information Science & Technology Body of Knowledge, *Web GIS Programming, Web GIS Programming Languages*. Retrieved at 22.03.2022, from: <https://gistbok.ucgis.org/bok-topics/web-gis-programming>
- Tempfli K. & Kerle N. & Huurneman G.C. & Janssen L.L.F (2009). Hengelosestraat 99, P.O. Box 6, 7500 AA Enschede, The Netherlands, Principles of Remote Sensing p279-299, *unsupervised image classification*. Retrieved at 18.03.2022, from: [https://webapps.itc.utwente.nl/librarywww/papers\\_2009/general/PrinciplesRemoteSensing.pdf#page=291](https://webapps.itc.utwente.nl/librarywww/papers_2009/general/PrinciplesRemoteSensing.pdf#page=291)

- The European Space Agency (esa), (February 3, 2022). *New Landsat 8 Collection-2 Level 1 and Level 2 data now available*. Retrieved at 02.04.2022, from: <https://earth.esa.int/eogateway/news/new-landsat-8-collection-2-level-1-and-level-2-data-now-available>
- Tiwari A. & Dr.Jain K. (November, 2013). GEOSPATIAL FRAMEWORK FOR DENGUE USING OPEN SOURCE WEB GIS TECHNOLOGY, *WEB GIS ARCHITECTURE*. Retrieved at 05.05.2022, from: <https://www.researchgate.net/publication/266738880>
- Tumelienė E. & Visockienė J.S. & Malienė, (June 20, 2021). The Influence of Seasonality on the Multi-Spectral Image Segmentation for Identification of Abandoned Land, *Image Segmentation Methods*, pp.6-8. Retrieved at 04.05.2022, from: <https://www.mdpi.com/2071-1050/13/12/6941/htm>
- UN-habitat, (June, 2014). Lattakia (City Profile Lattakia Multi Sector Assessment), *Governorate context, Geographic Typologies*. Retrieved at 06.03.2022, from: <https://www.alnap.org/system/files/content/resource/files/main/Lattakia%20%283%29.pdf>
- United Nations, Office for Outer Space Affairs UN-SPIDER Knowledge Portal (2022). Normalized Burn Ratio (NBR), *Normalized Burn Ratio (NBR), Burn Severity*. Retrieved at 16.4.2022, from: <https://un-spider.org/advisory-support/recommended-practices/recommended-practice-burn-severity/in-detail/normalized-burn-ratio>
- USGS, (2022). Landsat Missions, *Landsat Normalized Burn Ratio*. Retrieved at 12.04.2022, from: <https://www.usgs.gov/landsat-missions/landsat-normalized-burn-ratio>
- USGS, (2022). FAQ: *What is remote sensing and what is it used for?*. Retrieved at 13.03.2022, from: <https://www.usgs.gov/faqs/what-remote-sensing-and-what-it-used>
- USGS, (January 30, 2008). FAQ: *What are Landsat 7 SLC-off Gap Mask files?*. Retrieved at 12.03.2022, from: <https://www.usgs.gov/faqs/what-are-landsat-7-slc-gap-mask-files>
- USGS, (January 30, 2008). LANDSAT MISSIONS, Landsat 7, *Landsat 7 Scan Line Corrector (SLC) Failure*. Retrieved at 08.03.2022, from: <https://www.usgs.gov/landsat-missions/landsat-7>

USGS, (November 12, 2021). FAQ: *What are the band designations for the Landsat satellites?*. Retrieved at 11.03.2022, from: <https://www.usgs.gov/faqs/what-are-band-designations-landsat-satellites>

Veraverbeke S. & Lhermitte S. & Verstraeten W.W. & Goossens R. (May 24, 2010). The temporal dimension of differenced Normalized Burn Ratio (dNBR) fire/burn severity studies: The case of the large 2007 Peloponnese wild fires in Greece, pp.2549, *Introduction*. Retrieved at 12.04.2022, from: [http://www.earthmapps.io/pubs/2010\\_Veraverbeke\\_RSE\\_The%20temporal%20dimension%20of%20differenced.pdf](http://www.earthmapps.io/pubs/2010_Veraverbeke_RSE_The%20temporal%20dimension%20of%20differenced.pdf)

VizExperts (2022). WebGIS, *What is WebGIS, How does it work and what are its applications?* Retrieved at 21.3.2022, from: <https://vizexperts.com/webgis/>

Volodymyr Agafonkin, (April 4, 2022). Leaflet, *Overview*. Retrieved at 02.05.2022, from: <https://leafletjs.com/>

Wasser L. & Cattau M., (March 13, 2020). Lesson 4. Work with the Difference Normalized Burn Index - Using Spectral Remote Sensing to Understand the Impacts of Fire on the Landscape, *Calculate Normalized Burn Ratio (NBR), NBR Bands, Difference NBR* . Retrieved at 15.4.2022, from: <https://www.earthdatascience.org/courses/earth-analytics/multispectral-remote-sensing-modis/normalized-burn-index-dNBR/>

Wikipedia, (November 25, 2008). *Landsat-7.jpg*. Retrieved at 07.03.2022, from: <https://hu.m.wikipedia.org/wiki/F%C3%A1jl:Landsat-7.jpg>

## Abbreviations:

APIs	Applications Programming Interfaces
CSS	Cascading Style Sheets
dNBR	difference Normalized Burn Ratio
EROS	Earth Resources Observation and Science
ETM+	Enhanced Thematic Mapper Plus
GIS	Geographic Information System
HTML	Hypertext Markup Language
HTTP	Hypertext Transfer Protocol
JSON	JavaScript Object Notation
LDCM	Landsat Data Continuity Mission
LULC	Land Use Land Cover
NASA	National Aeronautics and Space Administration
NOAA	National Oceanic and Atmospheric Administration
OLI	Operational Land Imager
OTP	Orfeo Toolbox
SARC	Syrian Arab Red Crescent
SLC	Scan Line Corrector
TIRS	Thermal Infrared Sensor
URL	<i>Uniform Resource Locator</i>
USGS	United States Geological Survey
UTM	Universal Transverse Mercator

## **Acknowledgement:**

First, I would like to send my special and unique thanks to Professor **Gede Mátyás**, who helped me step by step in this project every time I needed. Professor guided and instructed me in each obstacle, answered all my questions, and supported my ideas. His efforts and notes helped me finish this thesis without any pressure and circumstances.

In addition, I want to thank our honored professors and teachers in MSc Cartography. You helped us in every subject to understand it clearly, and gave us this big opportunity to expand our knowledge and skills from your experience through this specialization.

Moreover, special thanks to Professor **Jung András** for his notes during this thesis, and thanks to my professors, teachers and friends in Syria, who were beside me in all my life stages until now.

Last but not least, the root of this opportunity is Hungary, which accepted me to complete my MSc studies in Eötvös Loránd University, and I am very grateful for this university and I appreciate the experience I had in this wonderful country.

## DECLARATION

I, undersigned *Mohamed Hamoud* (NEPTUN CODE: *MZV5W9*), declare that the present master's thesis is my original intellectual product in full and that I have not submitted any part or the whole of this work to any other institution. Permissions related to the use of copyrighted sources in this work are attached.

I AGREE to the publication of the accepted master's thesis in pdf form on the website of the Institute of Cartography and Geoinformatics.

Budapest, *15, May, 2022*

  
\_\_\_\_\_  
(signature of the student)